

Diffusion caused by two noises - active and thermal

Koushik Goswami¹ and K L Sebastian^{1,2}

¹*Department of Inorganic and Physical Chemistry,
Indian Institute of Science, Bangalore 560012, India*

²*Indian Institute of Technology Palakkad, Ahalia Integrated Campus,
Kozhippara 678557, Palakkad, Kerala, India*

Abstract

The diffusion of colloids inside an active system - *e.g.*, within a living cell or the dynamics of active particles itself (*e.g.*, self-propelled particles) can be modeled through overdamped Langevin equation which contains an additional noise term apart from the usual white Gaussian noise, originating from the thermal environment. The second noise is referred to as “active noise” as it arises from activity such as chemical reactions. The probability distribution function (PDF or the propagator) in space-time along with moments provides essential information for understanding their dynamical behavior. Here we employ the phase-space path integral method to obtain the propagator, thereby moments and PDF for some possible models for such noise. At first, we discuss the diffusion of a free particle driven by active noise. We consider four different possible models for active noise, to capture the possible traits of such systems. We show that the PDF for systems driven by noises other than Gaussian noise largely deviates from normal distribution at short to intermediate time scales as a manifestation of out-of-equilibrium state, albeit converges to Gaussian distribution after a long time as a consequence of the central limit theorem. We extend our work to the case of a particle trapped in a harmonic potential and show that the system attains steady state at long time limit. Also, at short time scales, the nature of distribution is different for different noises, *e.g.*, for particle driven by dichotomous noise, the probability is mostly concentrated near the boundaries whereas a long exponential tail is observed for a particle driven by Poissonian white noise.

CONTENTS

I. Introduction	3
II. The phase-space path integral for a particle subject to two noises	5
A. The free particle	7
B. Particle in a harmonic trap	8
III. Free particle subject to different types of noises $\sigma(t)$	8
A. Gaussian colored Noise	8
B. Dichotomous Poisson Noise	9
C. Poissonian White Noise	12
1. Short time limit	16
2. Long time limit	17
D. $\sigma(t)$ is taken as the position coordinate of an overdamped harmonic oscillator driven by Poissonian noise	
1. $\tilde{T} \ll 1$ and \tilde{x}_f arbitrary.	23
2. Long time ($\tilde{T} \gg 1$), large \tilde{x}_f ($\tilde{x}_f \gg 1$) limit.	23
3. Different time limits, but small \tilde{x}_f	24
IV. Results for harmonic oscillator in different types of noises $\sigma(t)$	28
A. Gaussian colored Noise	28
B. Dichotomous Poisson Noise	28
1. $\epsilon_A \gg 1$.	31
2. $\epsilon_A \ll 1$.	31
3. $\alpha \gg 1$.	31
4. $\alpha \ll 1$.	32
5. $\alpha = 2$.	34
C. Poissonian White Noise	34
1. Short time ($\tilde{T} \ll 1$).	36
2. Intermediate time.	37
3. Long time, $\tilde{T} \gg 1$.	39
V. Conclusion	40

VI. Acknowledgments	43
A. Limiting forms of PDF in the case where the active noise is dichotomous	43
a. Small time limit	44
b. Long time limit	45
B. Moments of $\sigma_{PC}(t)$ and its expression in terms of $\sigma_{PW}(t)$	46
C. Calculation of stationary probability distribution function for $\tilde{\tau} = 0.5$	47
References	47

I. INTRODUCTION

The dynamics of a colloidal particle in an environment of fast-moving solvent molecules is well described by the theory of Brownian motion formulated by Einstein in 1905 [1, 2]. The motion of the particle is random as it results from a large number of erratic collisions with the much smaller solvent molecules. The random force exerted by these molecules is uncorrelated at the timescale of relaxation of the particle and hence one usually models it as white, Gaussian noise (or thermal noise). Two interesting features of the resulting motion are: (a) the mean square displacement of the particle is proportional to the time spent by the particle in the environment and (b) the distribution of the particle’s displacement is Gaussian (this follows from the central limit theorem) [3]. In the recent past, situations where other types of noises, usually known as non-thermal noise, too act on the particle have attracted quite a bit of attention. For example, in a living cell the cytosol is mainly composed of inter-linked network system (*e.g.* actin filaments) and motor proteins (*e.g.* myosin II). With the consumption of ATP, the motors generate relative motion between the filaments resulting in random thrusts upon a particle residing inside the cell matrix. Such non-thermal noise, often termed as active noise, drives the system out of equilibrium. Contrary to thermal noise, such noise does not obey the fluctuation-dissipation theorem [4]. Recently, several experiments [5–7] have studied the dynamics of a tracer particle (*in vitro* as well as *in vivo*) in the cellular environment. In such experiments the fluctuations in spatial distribution of a probe particle placed inside the “active gel” was studied using video microrheology. For all the cases studied, the spatial distribution largely deviates from the normal distribution.

Many a times, an exponential tail with a central Gaussian part [5, 8] has been observed. Such behavior can be ascribed to a process driven by Poisson noise and thereby cytoplasmic matrix can be regarded as Poissonian bath. Other than the noises which characterize the heat bath, a noise can be generated externally using some specific device. Such noise was introduced in the system in order to study non-equilibrium processes by Mestres *et al.* [9]. The noise had finite correlation time and hence it can be modeled as colored Gaussian noise (Ornstein-Uhlenbeck process) or as dichotomous noise. It may also be noted that dichotomous noise has a wide range of applicability, and has been used to model various physical processes such as stochastic resonance [10–12], synchronization effects [13, 14], patterning [15, 16], thermally activated transition between two states etc [17]. Zheng *et. al* [18], studied the motion of micron-sized spherical Pt-silica Janus particles in H_2O_2 solution. They found that the probability distribution function for the displacement, deviates from Gaussianity under the experimental conditions, and the distribution is either a broadened peak or two-peaked structure depending upon the concentration of H_2O_2 . They formulated a theoretical model by considering a Langevin equation with coupled translational and rotational motion. However one can circumvent the rotational degrees of freedom by replacing it with dichotomous noise. Recently Malakar *et al.* have described a one dimensional version of the bacterial ‘Run and Tumble motion’(RTP) through a overdamped Langevin dynamics by adding an extra noise term [19]. In simplified 1D model, a bacteria can have either a state with $+u$ velocity or with $-u$, and the flip between these states is assumed to happen according to Poisson statistics. Not surprisingly, the extra noise has been considered as dichotomous. Apart from bacterial motion, two state models have been invoked extensively in the context of gene expression [20–27]. In particular, see Ref. [27] in which the impact of gene switching on production of mRNA during transcription has been studied. Depending on the binding or unbinding of promoters to specific DNA sites, gene can switch stochastically between two states, namely, active and inactive, and the randomness arising due to such transitions has been modeled as dichotomous noise. Akin to this, switching between discrete environmental states is pertinent in the study of predator-prey model [28–30], evolution theory [31, 32], bacterial population growth [33, 34] etc. Now coming to the non-equilibrium fluctuation in diffusion process, there have been a large number of experiments as well as theoretical investigations on confined particles. For example, in Ref. [35], the dynamics of an optically trapped Brownian particle coupled, to a bacterial bath has been studied to find

that it exhibits non-Boltzmann (more specifically, heavy-tailed) stationary distribution in strong confinement regime, contrary to the force-free case. However, for weak trapping and low concentration of bacteria the distribution becomes Gaussian with an enhanced variance and thus in this regime, force generated due to self-propulsion of bacteria acting on the passive particle can be taken to be correlated Gaussian noise [36]. Another example is the run-and-tumble particles confined in a restricted region, which happen to accumulate near boundaries of the geometry [37–39]. Driven systems have found applications in other fields too, *e.g.* in hydrology to model soil water balance [40], in ecology to describe the occurrence of fires in ecosystem [41] etc. Therefore it is of a great interest to calculate the time evolution of the probability distribution function (PDF), for a system that is subject to thermal noise (or immersed in a thermal bath), and is additionally driven by non-thermal noise. The common method for this purpose is to set up and solve the Fokker-Planck equation (FPE) describing the process [19]. There have been some approximate as well as exact solutions of the Fokker-Planck equations corresponding to the processes driven by Poisson white noise, Lévy stable noise and colored noise [42, 43]. However, the dynamical description for a system driven by two noises has not been explored in the full space-time range. Moreover, it is not always easy, particularly for colored noise, to solve the FPE and get the PDF analytically. Hence in this paper, we devise a general scheme to cover a large set of noises by employing the phase-space path integral approach [44, 45]. Further we investigate several dynamical systems corresponding to a wide class of physical processes, by assuming different noise models, and obtain their dynamical features at transient and steady states. Finally, we summarize our findings in the Section V.

II. THE PHASE-SPACE PATH INTEGRAL FOR A PARTICLE SUBJECT TO TWO NOISES

A particle undergoing usual Brownian motion in a potential $U(x)$ is described by the equation

$$\zeta \frac{dx(t)}{dt} = -U'(x) + f(t), \quad (1)$$

where the noise $f(t)$ is assumed to be Gaussian white noise having $\langle f(t) \rangle = 0$ and $\langle f(t)f(t') \rangle = 2k_B T \zeta \delta(t - t')$. The best way to characterize the noise $f(t)$ is through its probability density functional $\Psi[f(t)] \sim e^{-\frac{1}{4\zeta k_B T} \int dt f(t)^2}$. The diffusion coefficient of the

particle D is related to the coefficient of friction by $D = k_B T / \zeta$. It is convenient to rewrite the above as

$$\frac{dx(t)}{dt} = -V'(x) + \eta(t), \quad (2)$$

with $V(x) = U(x)/\zeta$ and $\eta(t) = f(t)/\zeta$ so that $\langle \eta(t)\eta(t') \rangle_{\eta(t)} = 2D\delta(t-t')$. The noise $\eta(t)$ has the characteristic functional [44]

$$\left\langle e^{i \int_0^T p(t)\eta(t)dt} \right\rangle_{\eta(t)} = e^{-D \int_0^T p(t)^2 dt}, \quad (3)$$

where $\langle \dots \rangle_{\eta(t)}$ denotes the average over all possible realizations of the noise $\eta(t)$.

Now consider a situation where the particle is subjected to an additional noise $\sigma(t)$, due to the presence of active particles in the system or some other physical process. This modifies Eq. (2) to

$$\frac{dx(t)}{dt} = -V'(x) + \eta(t) + \sigma(t). \quad (4)$$

Using the characteristic functional of Eq. (3), one can express the probability density functional $P[\eta(t)]$ as its functional Fourier transform:

$$P[\eta] = \int Dp e^{-D \int_0^T p(t)^2 dt} e^{-i \int_0^T p(t)\eta(t)dt}. \quad (5)$$

Using Eq. (4) one can rewrite $P[\eta(t)]$ as a functional of $x(t)$ (for more details the reader is referred to [45]), to get the probability density functional for any path $x(t)$ of the particle, in the interval $t \in [0, T]$.

$$P[x] = \int Dp e^{-D \int_0^T p(t)^2 dt} e^{-i \int_0^T p(t)(\dot{x}(t)+V'(x))dt} e^{i \int_0^T p(t)\sigma(t)dt}. \quad (6)$$

Note that as in [44, 45], we assume the Ito discretization of Eq. (4) as a result of which the Jacobian of the transformation $\eta(t) \rightarrow x(t)$ is just a constant. As the particle is not only driven by $\eta(t)$ but also by $\sigma(t)$, one has to consider all the realizations of $\sigma(t)$ over the time period of T . Performing average over these, leads to

$$P[x] = \int Dp e^{-D \int_0^T p(t)^2 dt} e^{-i \int_0^T p(t)(\dot{x}(t)+V'(x))dt} \left\langle e^{i \int_0^T p(t)\sigma(t)dt} \right\rangle_{\sigma(t)}. \quad (7)$$

For simplicity of notation, we have used $P[x]$ itself to denote the averaged quantity. Therefore, the probability of finding the particle at position x_f after time T provided it started at the position x_0 at the time $t = 0$ is given by

$$\mathbb{P}(x_f, T; x_0, 0) = \int_{x(0)=x_0}^{x(T)=x_f} Dx \int Dp e^{-D \int_0^T p(t)^2 dt} e^{-ip_T x_f + ip_0 x_0} e^{i \int_0^T (x(t)\dot{p}(t) - V'(x)p(t)) dt} \times \left\langle e^{i \int_0^T p(t)\sigma(t) dt} \right\rangle_{\sigma(t)}. \quad (8)$$

In Eq. (8), the functional integration is to be performed over all paths that start at x_0 at the time $t = 0$ and end at x_f at the time $t = T$. In cases where the potential $V(x)$ is at the most quadratic, the path integration over x can be performed easily (see [45] for more details) resulting in a Dirac delta functional involving $p(t)$. The delta functional makes the path integration over $p(t)$ easy to perform. The final result can be expressed as single integration over the value of p at the time T , $p_T (= p(T))$. We note that the same technique can be applied in underdamped limit and in that case path integration over $p(t)$ becomes a double integration over p_T and $p_0 (= p(0))$. As we will be using this procedure in the paper, we illustrate it for a free particle subject to the two noises.

A. The free particle

Putting $V(x) = 0$ in Eq. (8) we get the propagator for free particle as

$$\mathbb{P}(x_f, T; x_0, 0) = \int_{x(0)=x_0}^{x(T)=x_f} Dx \int Dp e^{-D \int_0^T p(t)^2 dt} e^{-ip_T x_f + ip_0 x_0} e^{i \int_0^T x(t)\dot{p}(t) dt} \mathcal{C}[p(t)] \quad (9)$$

where $\mathcal{C}[p(t)]$ is the characteristic functional for the noise $\sigma(t)$ defined by

$$\mathcal{C}[p(t)] = \left\langle e^{i \int_0^T p(t)\sigma(t) dt} \right\rangle_{\sigma(t)}. \quad (10)$$

As $\int_{x(0)=x_0}^{x(T)=x_f} Dx e^{i \int_0^T x(t)\dot{p}(t) dt} = \delta[\dot{p}(t)]$, where $\delta[\dots]$ is the Dirac delta functional, we get $\dot{p}(t) = 0$ and hence $p(t) = p_T = p_0$. Thus the path integral over $p(t)$ in Eq. (9) reduces to a single integration with respect to p_T . The propagator for the free particle becomes (after putting in appropriate normalization factor)

$$\mathbb{P}(x_f, T; x_0, 0) = \frac{1}{2\pi} \int_{-\infty}^{+\infty} dp_T e^{-D p_T^2 T} e^{-ip_T x_f + ip_T x_0} C(p_T), \quad (11)$$

where the function $C(p_T)$ is defined by $C(p_T) = \mathcal{C}[p(t)]_{p(t) \equiv p_T}$.

B. Particle in a harmonic trap

In this subsection, we analyze the dynamics of a particle bound in a harmonic potential $V(x) = \frac{1}{2}\lambda x^2$, where λ is the stiffness constant. In this case, the path integration over x in Eq. (8) can be performed and results in the delta functional $\delta[\dot{p}(t) - \lambda p(t)]$. This implies $\dot{p}(t) = \lambda p(t)$ which on solution gives $p(t) = p_T e^{\lambda(t-T)}$ where $p_T = p(T)$. Therefore the propagator for a harmonic oscillator becomes

$$\mathbb{P}(x_f, T; x_0, 0) = \frac{1}{2\pi} \int_{-\infty}^{+\infty} dp_T e^{-\frac{D p_T^2}{2\lambda}(1-e^{-2\lambda T}) - ip_T x_f + ip_0 x_0} G(p_T). \quad (12)$$

Here

$$G(p_T) = \mathcal{C}[p(t)]_{p(t) \equiv p_T e^{-\lambda(T-t)}} = \left\langle e^{ip_T \int_0^T e^{-\lambda(T-t)} \sigma(t) dt} \right\rangle_{\sigma(t)}. \quad (13)$$

Now if the initial distribution of the particle is $P(x_0)$, then one can get the probability distribution function for finding the particle at position x_f after time T , by integrating over all possible initial positions x_0 . Thus the probability distribution becomes

$$\mathbb{P}(x_f, T) = \int_{-\infty}^{+\infty} dx_0 \mathbb{P}(x_f, T; x_0, 0) P(x_0). \quad (14)$$

We now illustrate the method for several different choices of $\sigma(t)$.

III. FREE PARTICLE SUBJECT TO DIFFERENT TYPES OF NOISES $\sigma(t)$

A. Gaussian colored Noise

The simplest case that one can have is: $\sigma(t)$ is Gaussian colored noise $\sigma_{CG}(t)$ with zero mean. The correlation function is then given by $\langle \sigma_{CG}(t) \sigma_{CG}(t') \rangle = \frac{D_A}{\tau} e^{-\frac{|t-t'|}{\tau}}$. Using the cumulant expansion technique [1] one can find its characteristic functional to be

$$\left\langle e^{i \int_0^T p(t) \sigma_{CG}(t) dt} \right\rangle_{\sigma_{CG}(t)} = e^{-\frac{1}{2} \int_0^T \int_0^T p(t) p(t') \langle \sigma_{CG}(t) \sigma_{CG}(t') \rangle dt' dt}. \quad (15)$$

This gives

$$C(p_T) = e^{-p_T^2 D_A [T - \tau(1 - e^{-\frac{T}{\tau}})]}. \quad (16)$$

Using Eq. (16) in Eq. (11), one can get the probability distribution function

$$\mathbb{P}(x_f, T; x_0, 0) = \frac{e^{-\frac{(x_f - x_0)^2}{4T[D + D_A(1 - \frac{\tau}{T}(1 - e^{-\frac{T}{\tau}})])}}}{\sqrt{4\pi T[D + D_A(1 - \frac{\tau}{T}(1 - e^{-\frac{T}{\tau}})])}}. \quad (17)$$

Not surprisingly, the probability distribution is Gaussian with a mean squared displacement $\langle x^2(T) \rangle = 2T \left[D + D_A \left(1 - \frac{\tau}{T} (1 - e^{-\frac{T}{\tau}}) \right) \right]$. In the very small time limit (i.e., $T \ll \tau$), $\langle x^2(T) \rangle = 2DT$ showing that at such short time scales, the particle is moving with white noise-only diffusivity D . In the very large time limit, $\langle x^2(T) \rangle = 2(D + D_A)T$, implying that the diffusion has an effective diffusivity $D + D_A$. As the noises acting upon the particle are Gaussian in nature, it is natural to have Gaussian distribution of particle's position over any timescale of observation.

B. Dichotomous Poisson Noise

As we have mentioned before, the motion of self-propelled particles (Janus microbead or bacteria) can be conceived through Eq. (4), considering $\sigma(t)$ as dichotomous Poissonian noise. We will denote such noise by $\sigma_{DP}(t)$. It takes only two values: $+u$ and $-u$. Further, it is assumed to have the correlation $\langle \sigma_{DP}(t)\sigma_{DP}(t') \rangle = u^2 e^{-\gamma|t-t'|}$, implying the noise has a finite correlation time equal to $1/\gamma$. Note that $D_A = u^2/\gamma$ has the dimension of diffusivity, and can be thought of as diffusivity under the dichotomous noise. The characteristic function for such noise is given by [46–48]

$$C(p_T) = \left\langle e^{ip_T \int_0^T \sigma_{DP}(t) dt} \right\rangle_{\sigma_{DP}(t)} = e^{-\frac{\gamma T}{2}} \left[\cosh \left(\frac{\gamma u T}{2} \right) + \frac{\gamma}{\gamma_u} \sinh \left(\frac{\gamma u T}{2} \right) \right], \quad (18)$$

where

$$\begin{aligned} \gamma_u &= \gamma \left[1 - \frac{4u^2 p_T^2}{\gamma^2} \right]^{\frac{1}{2}} && \text{if } \frac{4u^2 p_T^2}{\gamma^2} \leq 1, \\ &= \gamma \left[\frac{4u^2 p_T^2}{\gamma^2} - 1 \right]^{\frac{1}{2}} \frac{p_T}{|p_T|} && \text{otherwise.} \end{aligned} \quad (19)$$

Using Eq. (18) in Eq. (11) one can get the PDF:

$$\mathbb{P}(x_f, T; x_0 = 0, 0) = \frac{1}{2\pi} \int_{-\infty}^{+\infty} dp_T e^{-ip_T x_f} F(p_T), \quad (20)$$

where

$$F(p_T) = e^{-DT p_T^2} e^{-\frac{\gamma T}{2}} \left[\cosh \left(\frac{\gamma u T}{2} \right) + \frac{\gamma}{\gamma_u} \sinh \left(\frac{\gamma u T}{2} \right) \right]. \quad (21)$$

Here we have taken the initial position $x_0 = 0$ without any loss of generality. The Fourier transform of Eq. (20) can be written as a convolution. The m^{th} moment of the displacement at any instant can be evaluated easily, using

$$\langle x^m(T) \rangle = \left[(-i)^m \frac{d^m F(p_T)}{dp_T^m} \right]_{p_T=0}. \quad (22)$$

Using Eq. (21) and Eq. (22) we get

$$\langle x^2(T) \rangle = 2DT + \frac{2D_A}{\gamma}(-1 + T\gamma + e^{-T\gamma}). \quad (23)$$

We first consider the case $\gamma T \ll 1$. Then $\langle x^2(T) \rangle \approx 2DT + \gamma D_A T^2 = DT(2 + u^2 T/D)$. Two limits can now be distinguished. The first is when $1 \gg u^2 T/2D$, in which case $\langle x^2(T) \rangle \approx 2DT$, meaning that the motion is purely diffusive. The other is when $u^2 T/2D \gg 1$, leading to $\langle x^2(T) \rangle \approx u^2 T^2$, and the motion is ballistic in this limit. In the long time limit, $\langle x^2(T) \rangle = 2DT + 2D_A T$ and the motion is purely diffusive with a diffusivity $D + D_A$. Insight into the behavior of probability distribution can be gained from the fourth moment, through the non-Gaussian parameter (NGP) γ_{np} defined by

$$\gamma_{np} = \frac{\langle x^4(T) \rangle}{3 \langle x^2(T) \rangle^2} - 1. \quad (24)$$

For a Gaussian distribution γ_{np} is zero whereas the distribution which decays faster than Gaussian has negative γ_{np} value and slower decaying distribution has a positive γ_{np} . After calculating the moments from Eq. (18) and Eq. (22) and using them in Eq. (24) we have

$$\begin{aligned} \gamma_{np} &= \frac{5 - 2T\gamma - 4e^{-T\gamma}(1 + T\gamma) - e^{-2T\gamma}}{[T\gamma + \frac{D}{D_A}T\gamma + e^{-T\gamma} - 1]^2} \\ &= \frac{5 - 2\tilde{T} - 4e^{-\tilde{T}}(1 + \tilde{T}) - e^{-2\tilde{T}}}{[\tilde{T} + \frac{\tilde{T}}{\epsilon_A} + e^{-\tilde{T}} - 1]^2} \end{aligned} \quad (25)$$

We use the dimensionless variables, $\tilde{T} = \gamma T$, $\epsilon_A = \frac{D_A}{D}$ and have plotted γ_{np} in Fig. 1

For any finite value of ϵ_A , in both large and small time limits $\gamma_{np}(\tilde{T})$ approaches the value of zero indicating its Gaussian behavior. However, for $\epsilon_A \rightarrow \infty$ ($D \rightarrow 0$), $\gamma_{np}(0) = -2/3$ as in this limit only the dichotomous noise is important. In Fig. 1, the plot for $\epsilon_A = 1000$ exemplifies this kind of behavior. In this case the value of $\gamma_{np}(\tilde{T})$ increases with time, eventually attaining the value zero in the long time limit.

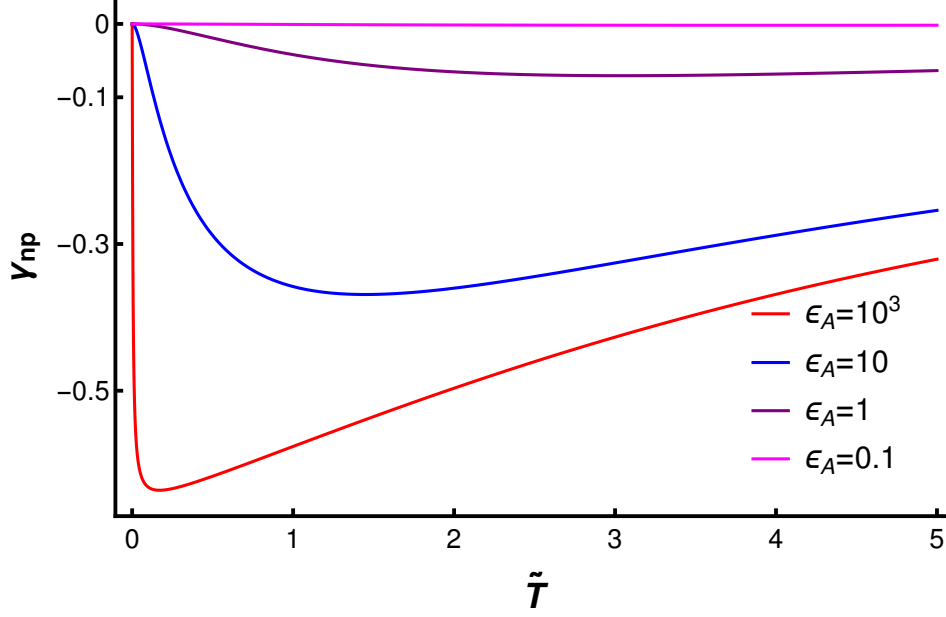


Figure 1. Dichotomous plus thermal noise: The non-Gaussian parameter (γ_{np}) is plotted against the dimensionless time \tilde{T} for different diffusivity ratios $\epsilon_A = D_A/D$.

$\gamma_{np}(\tilde{T})$ is always negative. This is essentially because the dichotomous noise makes the distribution non-Gaussian. Further, the fact that it is always negative means that the distribution is narrower than a Gaussian of the same $\langle x^2 \rangle$ value. To access the full description of the dynamics one is required to obtain PDF which is spatial Fourier inverse of $F(p_T)$. Obviously,

$$\mathbb{P}(x_f, T; 0, 0) = \int_{-\infty}^{+\infty} dx' F_1(x_f - x') F_2(x'), \quad (26)$$

where

$$F_1(x) = \frac{1}{2\pi} \int_{-\infty}^{+\infty} dp_T e^{ip_T x} e^{-DT p_T^2} = \frac{1}{\sqrt{4\pi DT}} e^{-\frac{x^2}{4DT}} \quad (27)$$

and

$$\begin{aligned} F_2(x) &= \frac{1}{2\pi} \int_{-\infty}^{+\infty} dp_T e^{ip_T x} e^{-\frac{\gamma T}{2}} \left[\cosh\left(\frac{\gamma_u T}{2}\right) + \frac{\gamma}{\gamma_u} \sinh\left(\frac{\gamma_u T}{2}\right) \right] \\ &= \frac{e^{-\frac{\gamma T}{2}}}{2} [\delta(x + uT) + \delta(x - uT)] \\ &\quad + \frac{\gamma}{4u} e^{-\frac{\gamma T}{2}} \left[I_0\left(\frac{\gamma T}{2} y\right) + \frac{1}{y} I_1\left(\frac{\gamma T}{2} y\right) \right] [\theta(x + uT) - \theta(x - uT)], \end{aligned} \quad (28)$$

where I_ν is the modified Bessel Function and $y = \sqrt{1 - \left(\frac{x}{uT}\right)^2}$.

Apart from the two dimensionless parameters \tilde{T} , ϵ_A , we now introduce another dimensionless quantity which is defined as: $\tilde{x} = x \frac{\tilde{T}}{u}$ and thereby we rewrite Eq. (26)-(28) in terms of them as follows:

$$\mathbb{P}(\tilde{x}_f, \tilde{T}; 0, 0) = \int_{-\infty}^{+\infty} d\tilde{x}' F_1(\tilde{x}_f - \tilde{x}') F_2(\tilde{x}'), \quad (29)$$

with

$$F_1(\tilde{x}) = \sqrt{\frac{\epsilon_A}{4\pi\tilde{T}}} e^{-\frac{\epsilon_A \tilde{x}^2}{4\tilde{T}}} \quad (30)$$

and

$$\begin{aligned} F_2(\tilde{x}) = & \frac{e^{-\frac{\tilde{x}}{2}}}{2} [\delta(\tilde{x} + \tilde{T}) + \delta(\tilde{x} - \tilde{T})] \\ & + \frac{1}{4} e^{-\frac{\tilde{x}}{2}} \left[I_0\left(\frac{\tilde{T}}{2}y\right) + \frac{1}{y} I_1\left(\frac{\tilde{T}}{2}y\right) \right] [\theta(\tilde{x} + \tilde{T}) - \theta(\tilde{x} - \tilde{T})] \end{aligned} \quad (31)$$

where $y = \sqrt{1 - \left(\frac{\tilde{x}}{\tilde{T}}\right)^2}$. These results are identical to those of Malakar *et al.* [19].

Further mathematical details are discussed in Appendix A. From Eq. (A7) one sees that during times lesser than the correlation time of dichotomous noise, the distribution function is centered around $\pm uT$ as shown in Fig. 2 (a). This is due to the fact that dichotomous noise itself can take up only two values $+u$ and $-u$, resulting particles to accumulate at those regions at initial stage. However in the case where strength of active noise is smaller compared to white noise these two peaks can not be distinguished as shown in Fig. 3. With the passage of time the distribution spreads as an effect of white noise as well as the active noise which causes an additional diffusivity D_A . After a very long time the distribution becomes Gaussian as given in Eq. (A11).

C. Poissonian White Noise

Here we consider $\sigma(t)$ as Poissonian white noise denoted by $\sigma_{PW}(t)$ - this means that the noise is generated by a random sequence of pulses at times t_i that follow Poisson distribution. We can express it as $\sigma_{PW}(t) = \sum_i a_i g(t - t_i)$, where $g(t - t_i)$ is the pulse centered at t_i which has an amplitude a_i . The probability of having n pulses in a time interval T is given by

$$P(n; \mu, T) = \frac{(\mu T)^n e^{-\mu T}}{n!}. \quad (32)$$

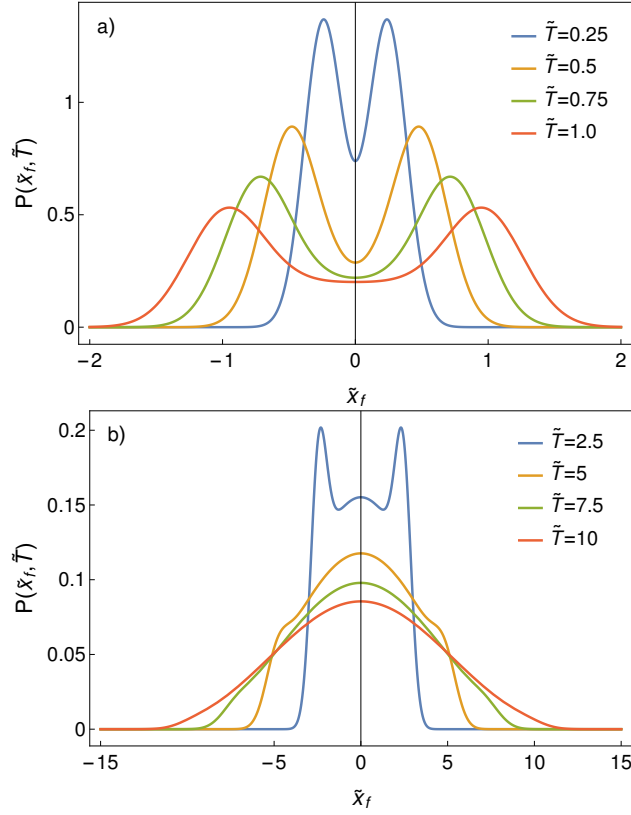


Figure 2. Dichotomous+thermal noise: The probability distribution function vs. displacement plot at (a) small \tilde{T} and (b) large \tilde{T} limit for high diffusivity ratio at $\epsilon_A = D_A/D = 25$.

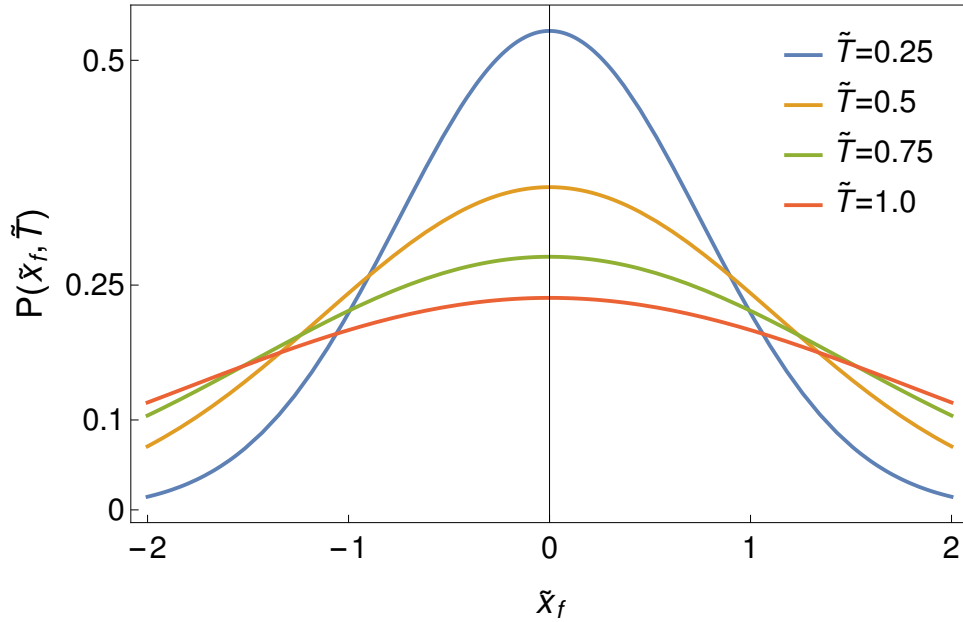


Figure 3. Dichotomous+white noise: The probability distribution function is plotted against displacement at different times for small diffusivity ratio at $\epsilon_A = D_A/D = 1$.

In the above, μ is the rate of the pulses. Usually $g(t - t_i)$ is assumed to be a delta function pulse and the amplitude a_i can take any value between $-\infty$ to $+\infty$. We assume it to be (double-)exponentially distributed (more specifically distributed according to the Laplace distribution). Hence the probability distribution of amplitude a , denoted as $P(a)$ can be expressed as

$$P(a) = \frac{1}{2a_0} e^{-\frac{|a|}{a_0}}, \quad (33)$$

where a_0 determines how broad the distribution of a is. The Poisson white noise has zero mean and delta correlation. That is,

$$\langle \sigma_{PW}(t_1) \sigma_{PW}(t_2) \rangle = 2\mu a_0^2 \delta(t_1 - t_2). \quad (34)$$

The strength of correlation, μa_0^2 can be regarded as diffusivity due to the Poisson noise and hence will be denoted as D_A .

Such noise can be characterized by its characteristic functional (see Ref. [49] for more information):

$$\left\langle e^{i \int_0^T q(s) \sigma_{PW}(s) ds} \right\rangle_{\sigma_{PW}(s)} = \exp \left[-\mu \int_0^T \frac{a_0^2 q(s)^2}{1 + a_0^2 q(s)^2} ds \right]. \quad (35)$$

To get the PDF from the Eq. (11), one is required to know the characteristic function which is obtained in this case from Eq. (35) and it is

$$C(p_T) = \exp \left(-\frac{T}{\tau_A} \frac{a_0^2 p_T^2}{1 + a_0^2 p_T^2} \right). \quad (36)$$

Here the characteristic time scale τ_A for active noise is the inverse of Poisson rate, *i.e.*, $\tau_A = \frac{1}{\mu}$. Therefore, the PDF can be expressed as

$$\mathbb{P}(x_f, T; x_0 = 0, 0) = \frac{1}{2\pi} \int_{-\infty}^{+\infty} dp_T e^{-ip_T x_f} e^{-DT p_T^2 - \frac{T}{\tau_A} \frac{a_0^2 p_T^2}{1 + a_0^2 p_T^2}}. \quad (37)$$

The MSD is calculated using the relation (22) and is given by: $\langle x(T)^2 \rangle = 2DT + 2D_A T$.

So the dynamics is always Fickian. The non-Gaussian parameter (γ_{np}) is computed from Eq. (24) using Eq. (37) and it is given by

$$\gamma_{np} = \frac{2a_0^2 D_A}{T(D + D_A)^2} = \frac{2\epsilon_A^2}{\tilde{T}(1 + \epsilon_A)^2}, \quad (38)$$

where $\tilde{T} = T/\tau_A$ is the dimensionless time and $\epsilon_A = D_A/D$. Using Eq. (38) we have made a plot of non-Gaussian parameter (γ_{np}) as a function of scaled time \tilde{T} as shown in Fig. 4. One can observe that at very large time limit γ_{np} decays to zero evincing its convergence

towards the Gaussian distribution. However in the very small time limit the distribution is not Gaussian as γ_{np} is non-zero. But it decays to zero very rapidly for the case where normal diffusivity is very high in magnitude compared to active diffusivity. It is interesting to note that in comparison with the dichotomous noise considered in the previous section, for this process $\gamma_{np}(t)$ is always positive. This means that the distribution is always broader than a Gaussian distribution and eventually reaches Gaussian in the long time limit. This happens only slowly, as $\gamma_{np} \propto 1/\tilde{T}$.

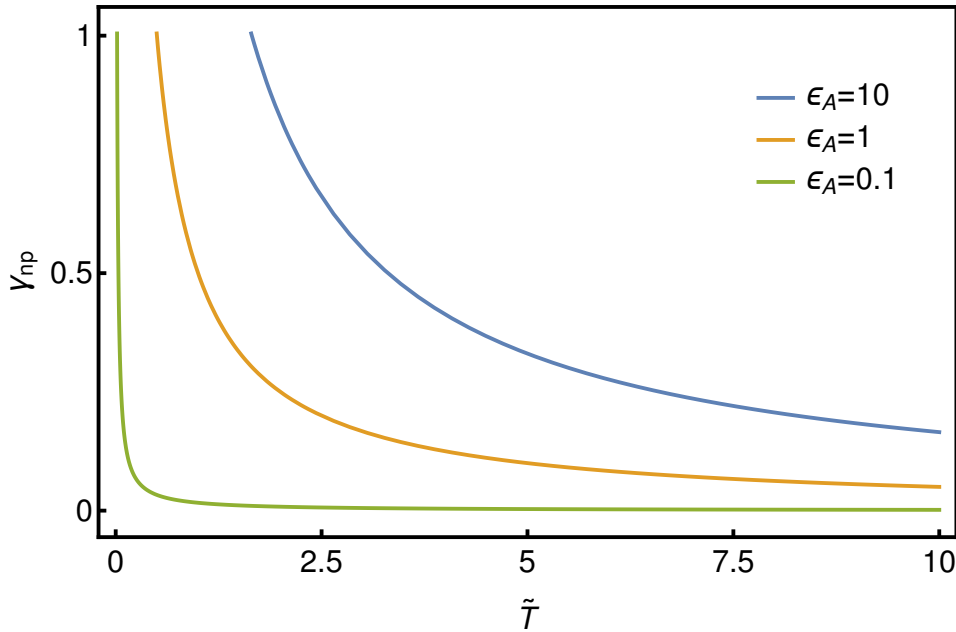


Figure 4. Gaussian+Poissonian white noises: the non-Gaussian parameter (γ_{np}) is plotted against the rescaled time \tilde{T} for different values of $\epsilon_A = D_A/D$.

We will now find the short time and long time limits of the PDF. Considerable insight into the nature of PDF is gained from rewriting the probability distribution as in Eq. (41). For this, we scale the variables into dimensionless quantities as: $\tilde{x}_f = \frac{x_f}{a_0}$, $\tilde{p}_T = a_0 p_T$ and

write the Eq. (37) as

$$\mathbb{P}(\tilde{x}_f, \tilde{T}; \tilde{x}_0 = 0, 0) = \frac{1}{2\pi} \int_{-\infty}^{+\infty} d\tilde{p}_T e^{-i\tilde{p}_T \tilde{x}_f} e^{-\frac{D}{D_A} \frac{T}{\tau_A} \tilde{p}_T^2 - \frac{T}{\tau_A} (1 - \frac{1}{1 + \tilde{p}_T^2})} \quad (39)$$

$$= \frac{1}{2\pi} \int_{-\infty}^{+\infty} d\tilde{p}_T e^{-i\tilde{p}_T \tilde{x}_f} e^{-\frac{\tilde{T}}{\epsilon_A} \tilde{p}_T^2 - \tilde{T}} \sum_{n=0}^{\infty} \frac{1}{n!} \left(\frac{\tilde{T}}{1 + \tilde{p}_T^2} \right)^n \quad (40)$$

$$= \frac{1}{2\pi} \int_{-\infty}^{+\infty} d\tilde{p}_T e^{-i\tilde{p}_T \tilde{x}_f} e^{-\frac{\tilde{T}}{\epsilon_A} \tilde{p}_T^2 - \tilde{T}} + Q$$

$$= \frac{\sqrt{\epsilon_A}}{\sqrt{4\pi\tilde{T}}} e^{-\tilde{T} - \tilde{x}_f^2 \epsilon_A / (4\tilde{T})} + Q. \quad (41)$$

In the above,

$$Q = \frac{1}{2\pi} \int_{-\infty}^{+\infty} d\tilde{p}_T e^{-i\tilde{p}_T \tilde{x}_f} e^{-\frac{\tilde{T}}{\epsilon_A} \tilde{p}_T^2 - \tilde{T}} \sum_{n=1}^{\infty} \frac{1}{n!} \left(\frac{\tilde{T}}{1 + \tilde{p}_T^2} \right)^n. \quad (42)$$

One can use the convolution theorem (Eq. (26)) as the following Fourier transforms are well known:

$$\int_{-\infty}^{+\infty} d\tilde{p}_T \frac{e^{i\tilde{p}_T x_f}}{(1 + \tilde{p}_T^2)^\nu} = \frac{2^{\frac{3}{2}-\nu} \sqrt{\pi} |\tilde{x}_f|^{\nu-\frac{1}{2}} K_{\nu-\frac{1}{2}}(|\tilde{x}_f|)}{\Gamma(\nu)} \quad (43)$$

and

$$\int_{-\infty}^{+\infty} d\tilde{p}_T e^{i\tilde{p}_T(\tilde{x}_f-x)} e^{-\frac{\tilde{T}}{\epsilon_A} \tilde{p}_T^2} = \sqrt{\frac{\epsilon_A}{4\pi\tilde{T}}} e^{-\frac{\epsilon_A(\tilde{x}_f-x)^2}{4\tilde{T}}}, \quad (44)$$

where $K(x)$ is Modified Bessel function of second kind [50]. Then one gets

$$\mathbb{P}(\tilde{x}_f, \tilde{T}; \tilde{x}_0 = 0, 0) = \sqrt{\frac{\epsilon_A}{4\pi\tilde{T}}} e^{-\tilde{T} - \epsilon_A \tilde{x}_f^2 / (4\tilde{T})}$$

$$+ \frac{1}{2\pi} \sum_{n=1}^{\infty} \frac{e^{-\tilde{T}}}{n!} (\tilde{T})^n \int_{-\infty}^{\infty} dx \frac{2^{\frac{3}{2}-n} \sqrt{\pi} |\tilde{x}|^{n-\frac{1}{2}} K_{n-\frac{1}{2}}(|\tilde{x}|)}{\Gamma(n)} \sqrt{\frac{\epsilon_A}{4\pi\tilde{T}}} e^{-\epsilon_A(\tilde{x}_f-x)^2 / (4\tilde{T})}, \quad (45)$$

which is an exact expression for the probability distribution function. We use this to demonstrate that the PDF would have an exponential (and not Gaussian) tail in the appropriate limits.

1. Short time limit

We now consider the limit where active noise is the dominant effect - i.e., the displacement due to the thermal noise is much smaller than the average jump due to active noise, i.e., $\epsilon_A/\tilde{T} \gg 1$. Then, one can evaluate the convolution integral by approximating $\sqrt{\frac{\epsilon_A}{4\pi\tilde{T}}} e^{-\epsilon_A(\tilde{x}_f-x)^2 / (4\tilde{T})} \approx \delta(\tilde{x}_f - x)$. In the large \tilde{x}_f limit, (i.e., $\tilde{x}_f \gg 1$), one can use the

asymptotic form for the Bessel function $K_n(|\tilde{x}_f|) \approx \sqrt{\frac{\pi}{2|\tilde{x}_f|}} e^{-|\tilde{x}_f|}$. With this, the sum on the right-hand side of Eq. (45) can be performed to get

$$\mathbb{P}(\tilde{x}_f, \tilde{T}; \tilde{x}_0 = 0, 0) = \sqrt{\frac{\epsilon_A}{4\pi\tilde{T}}} e^{-\tilde{T} - \epsilon_A \tilde{x}_f^2 / (4\tilde{T})} + \frac{e^{-|\tilde{x}_f| - \tilde{T}}}{2} \sqrt{\frac{2\tilde{T}}{|\tilde{x}_f|}} I_1\left(\sqrt{2\tilde{T}|\tilde{x}_f|}\right), \quad (46)$$

where I_1 is the modified Bessel function of the first kind [50]. In the limit that we have just considered, it is clear that the first term on the RHS can be neglected. For times such that $2\tilde{T}|\tilde{x}_f| \gg 1$, one can use the asymptotic expansion of $I_1(z) \approx \frac{e^z}{\sqrt{2\pi z}}$ to get

$$\mathbb{P}(\tilde{x}_f, \tilde{T}; \tilde{x}_0 = 0, 0) \approx \frac{\tilde{T}}{2\pi} \frac{e^{-|\tilde{x}_f| + \sqrt{2\tilde{T}|\tilde{x}_f|} - \tilde{T}}}{\left(2\tilde{T}|\tilde{x}_f|\right)^{\frac{3}{4}}}. \quad (47)$$

Therefore one can state that the distribution given in Eq. (46) consists of two terms - the first term manifests the Gaussian distribution whereas the second term does for exponential one. For the system with $D \ll D_A$, at very short time period it attains the condition: $x_f^2 \gg DT$ at very small displacement limit. Hence the distribution exhibits a prominent, long exponential tail. But for the system with $D \gg D_A$, the same condition is achieved at long displacement limit resulting in an insignificant exponential tail, which disappears quickly as time progresses. On the other hand Gaussian is dominant feature here as it decays very slowly. This result supports our previous analysis on non-Gaussian parameter.

We have performed numerical integration of Eq. (41) for two different values of ϵ_A and have made a plot of PDF as a function of dimensionless displacement \tilde{x}_f within a short time range \tilde{T} as shown in Fig. 5. For higher ϵ_A value the particle is distributed with an exponential tail at short time and position limits due to the fact that active diffusivity favors the exponential distribution over normal as depicted in Fig. 5(a). In case of small ϵ_A value the distribution is mostly Gaussian at short time and displacement region as pictorially illustrated in Fig. 5(b). The similarity of these to the experimentally observed probability distributions in [8] is very noticeable.

2. Long time limit

To get PDF at long time limit, using the identity

$$\left(\frac{\tilde{T}}{\tau_A(1 + \tilde{p}_T^2)}\right)^n = \left(\frac{\tilde{T}}{\tau_A}\right)^n \frac{1}{(n-1)!} \left\{ \left(-\frac{\partial}{\partial b}\right)^{n-1} \int_0^\infty d\alpha e^{-\alpha(b + \tilde{p}_T^2)} \right\}_{b=1}$$

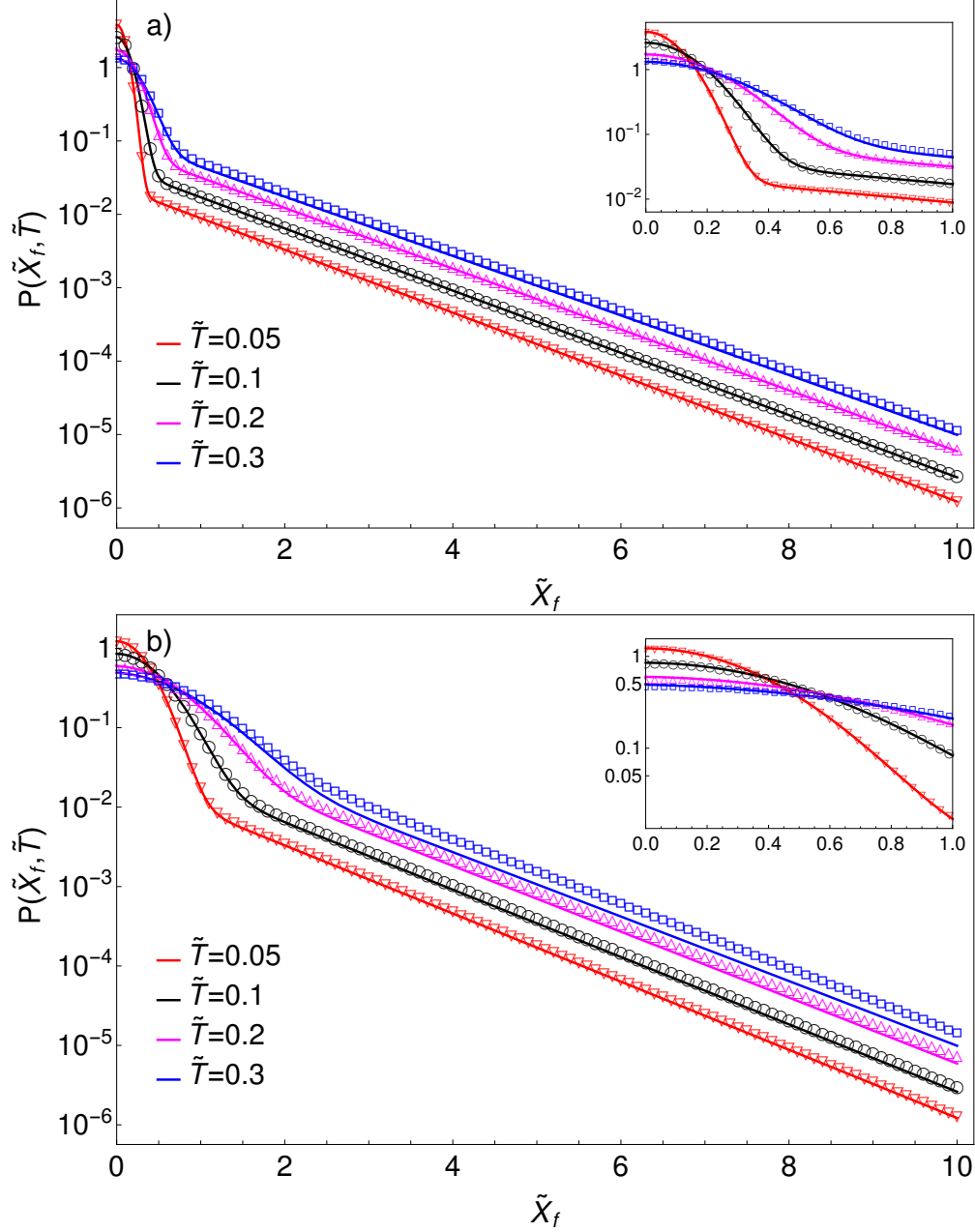


Figure 5. Gaussian+Poissonian white noises: logarithmic values of the probability distribution function are plotted against dimensionless displacement \tilde{x}_f at different scaled times \tilde{T} for two diffusivity ratios (a) $\epsilon_A = 10$ and (b) $\epsilon_A = 1.0$. The symbols are used for numerical values obtained after performing integration in Eq. (41) numerically. The solid curves represent Eq. (46) which is an analytical approximation valid at small time scale. From the plots it is seen that the approximation is quite good for $\tilde{T} \leq 0.1$. The existence of a Gaussian distribution at short \tilde{x}_f and an exponential one for large \tilde{x}_f is clearly seen.

we can write

$$Q = \frac{1}{2\pi} \frac{\tilde{T}}{\tau_A} \int_{-\infty}^{+\infty} d\tilde{p}_T e^{-i\tilde{p}_T \tilde{x}_f} e^{-\frac{\tilde{T} \tilde{p}_T^2}{\epsilon_A} - \tilde{T}} \\ \times \sum_{n=0}^{\infty} \frac{\tilde{T}^n}{(n+1)!n!} \left\{ \left(-\frac{\partial}{\partial b} \right)^n \int_0^{\infty} d\alpha e^{-\alpha(b+\tilde{p}_T^2)} \right\}_{b=1}.$$

This may be rewritten as

$$Q = e^{-\tilde{T}} \tilde{T} \int d\alpha \sum_{n=0}^{\infty} \frac{\alpha^n}{(n+1)!n!} \left(\tilde{T} \right)^n e^{-\alpha} \\ \times \frac{1}{2\pi} \int_{-\infty}^{\infty} d\tilde{p}_T e^{-i\tilde{p}_T \tilde{x}_f} e^{-(\frac{\tilde{T}}{\epsilon_A} + \alpha) \tilde{p}_T^2}.$$

On performing the sum and the integral over \tilde{p}_T , we get

$$Q = e^{-\tilde{T}} \tilde{T} \int_0^{\infty} d\alpha e^{-\alpha} \sqrt{\frac{1}{\tilde{T}\alpha}} I_1 \left(2\sqrt{\alpha\tilde{T}} \right) \frac{e^{-\frac{x_f^2}{4(\tilde{T}/\epsilon_A + \alpha)}}}{\sqrt{4\pi(\tilde{T}/\epsilon_A + \alpha)}}.$$

Changing the variable α to z defined by $\alpha = \tilde{T}z^2$ we can write the above as

$$Q = e^{-\tilde{T}} 2\tilde{T} \int_0^{\infty} dz e^{-\tilde{T}z^2} I_1(2\tilde{T}z) \frac{e^{-\frac{x_f^2}{4\tilde{T}(1/\epsilon_A + z^2)}}}{\sqrt{4\pi\tilde{T}(1/\epsilon_A + z^2)}}.$$

Using this in Eq. (41) gives

$$\mathbb{P}(\tilde{x}_f, \tilde{T}; \tilde{x}_0 = 0, 0) = \sqrt{\frac{\epsilon_A}{4\pi\tilde{T}}} e^{-\tilde{T} - \epsilon_A \tilde{x}_f^2 / (4\tilde{T})} \\ + e^{-\tilde{T}} 2\tilde{T} \int dz e^{-\tilde{T}z^2} I_1(2\tilde{T}z) \frac{e^{-\frac{\tilde{x}_f^2}{4\tilde{T}(1/\epsilon_A + z^2)}}}{\sqrt{4\pi\tilde{T}(1/\epsilon_A + z^2)}}. \quad (48)$$

Note that the probability distribution is explicitly written as the sum (integral) of a collection of Gaussians. Each Gaussian has a width proportional to \tilde{T} . Hence at any instant, the width of the distribution is proportional to \tilde{T} - implying that Fick's law is obeyed at all times. For large values of \tilde{T} one can neglect the first term, and can approximate $I_1(2\tilde{T}z)$ in the second term as $\approx e^{2\tilde{T}z} \sqrt{1/(4\pi\tilde{T}z)}$. This gives

$$\mathbb{P}(\tilde{x}_f, \tilde{T}; x_0 = 0, 0) = \sqrt{\frac{\tilde{T}}{\pi}} \int_0^{\infty} dz e^{-\tilde{T}(z-1)^2} \frac{e^{-\frac{x_f^2}{4\tilde{T}(1/\epsilon_A + z^2)}}}{\sqrt{4\pi\tilde{T}(1/\epsilon_A + z^2)}}$$

$e^{-\tilde{T}(z-1)^2}$ has its maximum value at $z = 1$. In the limit $\tilde{T} \rightarrow \infty$, one can hence replace z everywhere else by unity, and extend the lower limit of integration to $-\infty$. This gives

$$\begin{aligned} \mathbb{P}(\tilde{x}_f, \tilde{T}; x_0 = 0, 0) &= \frac{e^{-\frac{\tilde{x}_f^2}{4\tilde{T}(1+1/\epsilon_A)}}}{\sqrt{4\pi\tilde{T}(1+1/\epsilon_A)}} \sqrt{\frac{\tilde{T}}{\pi}} \int_{-\infty}^{\infty} d\xi e^{-\tilde{T}\xi^2} \\ &= \frac{e^{-\frac{\tilde{x}_f^2}{4\tilde{T}(1+1/\epsilon_A)}}}{\sqrt{4\pi\tilde{T}(1+1/\epsilon_A)}}. \end{aligned} \quad (49)$$

Hence in the long time limit, the result is a Gaussian with $\langle \tilde{x}_f^2 \rangle = 2(1+1/\epsilon_A)\tilde{T}$, as one would expect.

D. $\sigma(t)$ is taken as the position coordinate of an overdamped harmonic oscillator driven by Poissonian white noise.

In this section we will take the active noise $\sigma(t)$ to be correlated Poissonian, which we will denote by the symbol $\sigma_{PC}(t)$. As the generation of active force usually happens as a result of a Poisson process, we assume the active force $\sigma_{PC}(t)$ as the position coordinate of a harmonically bound fictitious particle driven by Poisson white noise $\sigma_{PW}(t)$. Hence its dynamics follows

$$\frac{d\sigma_{PC}(t)}{dt} = -\frac{1}{\tau_p}\sigma_{PC}(t) + \frac{1}{\tau_p}\sigma_{PW}(t), \quad (50)$$

where $\sigma_{PW}(t)$ has been defined in the previous section. We have shown in Appendix B that $\sigma_{PC}(t)$ has exponential correlation (see Eq. (B3)) and the associated timescale is correlation time, denoted as τ_p . We can write the characteristic functional of $\sigma_{PC}(t)$ in terms of Poisson noise $\sigma_{PW}(t)$ as (for details see Appendix B)

$$\left\langle e^{ip_T \int_0^T \sigma_{PC}(t) dt} \right\rangle = \left\langle e^{i \int_{-\infty}^{\infty} q(s) \sigma_{PW}(s) ds} \right\rangle_{\sigma_{PW}(s)}, \quad (51)$$

where

$$q(s) = p_T [\Theta(-s) e^{\lambda_p s} (1 - e^{-\lambda_p T}) + \Theta(s) \Theta(T-s) (1 - e^{-\lambda_p (T-s)})] \quad (52)$$

with $\lambda_p = 1/\tau_p$. $\Theta(t)$ is usual Heaviside theta function. Using Eq. (35) in Eq. (51) one can obtain the characteristic function

$$\begin{aligned} \left\langle e^{ip_T \int_0^T \sigma_{PC}(t) dt} \right\rangle_{\sigma_{PW}(t)} = & \exp \left[-\frac{\tau_p}{\tau_a} \frac{a_0 p_T}{1 + a_0^2 p_T^2} (a_0 \lambda_p T p_T - \tan^{-1}(a_0 \rho p_T)) \right] \\ & \times (1 + a_0^2 \rho^2 p_T^2)^{-\frac{\tau_p}{2\tau_a} \frac{a_0^2 p_T^2}{1 + a_0^2 p_T^2}}. \end{aligned} \quad (53)$$

Here, $\rho = 1 - e^{-T\lambda_p}$ and τ_a is inverse of Poisson rate μ (i.e., $\tau_a = \frac{1}{\mu}$), and is the characteristic timescale for the active noise. a_0 is the characteristic length scale of the active noise. We define the diffusivity due to the active noise as $D_A = \frac{a_0^2}{\tau_a}$.

Using Eq. (53) in Eq. (11), leads to the probability distribution function for finding the particle at the position x_f after a time T , given that it started at $x_0 = 0$ at time $T = 0$ as

$$\mathbb{P}(x_f, T; x_0 = 0, 0) = \frac{1}{2\pi} \int_{-\infty}^{+\infty} dp_T e^{-ip_T x_f} \mathbb{F}(p_T), \quad (54)$$

where

$$\mathbb{F}(p_T) = e^{-DT p_T^2} \exp \left[-\frac{\tau_p}{\tau_a} \frac{a_0 p_T}{1 + a_0^2 p_T^2} (a_0 \lambda_p T p_T - \tan^{-1}(a_0 \rho p_T)) \right] (1 + a_0^2 \rho^2 p_T^2)^{-\frac{\tau_p}{2\tau_a} \frac{a_0^2 p_T^2}{1 + a_0^2 p_T^2}}. \quad (55)$$

Using Eq. (22), the MSD is calculated from Eq. (55) to be

$$\langle x(T)^2 \rangle = 2DT + 2\frac{D_A}{\lambda_p} [T\lambda_p + e^{-T\lambda_p} - 1]. \quad (56)$$

In the small time limit ($\lambda_p T \ll 1$), $\langle x(T)^2 \rangle = 2DT$ suggesting that the motion of the particle is influenced by only white noise. At the intermediate time scale *i.e.* when $0 < \lambda_p T < 1$, it starts to feel the effect of active noise. In the large time limit ($\lambda_p T \gg 1$) it diffuses with an enhanced diffusivity $D + D_A$ as the MSD is given by $\langle x(T)^2 \rangle = 2(D + D_A)T$.

To get an inkling about the behavior of PDF at large displacement we have computed γ_{np} applying Eq. (24) and it is given by

$$\begin{aligned} \gamma_{np}(T) &= \frac{D_A a_0^2 [-11 + 6T\lambda_p + 18e^{-T\lambda_p} - 9e^{-2T\lambda_p} + 2e^{-3T\lambda_p}]}{3\tau_p [D_A(-1 + T\lambda_p + e^{-T\lambda_p}) + DT\lambda_p]^2} \\ &= \frac{\tilde{\tau} \epsilon_A^2 [-11 + 6\tilde{T} + 18e^{-\tilde{T}} - 9e^{-2\tilde{T}} + 2e^{-3\tilde{T}}]}{3 [\epsilon_A(-1 + \tilde{T} + e^{-\tilde{T}}) + \tilde{T}]^2}. \end{aligned} \quad (57)$$

Here we have expressed the $\gamma_{np}(\tilde{T})$ in terms of the dimensionless variables defined by $\tilde{T} = \frac{T}{\tau_p} = \lambda_p T$, $\tilde{\tau} = \frac{\tau_a}{\tau_p}$, $\epsilon_A = \frac{D_A}{D}$. At small and large times, $\gamma_{np}(T)$ vanishes indicating

Gaussian behavior of the probability distribution. At intermediate time scale, $\gamma_{np}(T)$ attains a maximum and then it slowly decays to zero in the long time limit as shown in Fig. 6. This suggests that the distribution deviates from Gaussianity significantly in the intermediate time range as before the particle samples around the local surroundings it is triggered by the active noise. As ϵ_A takes higher value, the peak height keeps increasing indicating that the active noise is responsible for the non-Gaussianity. Now the complete features of

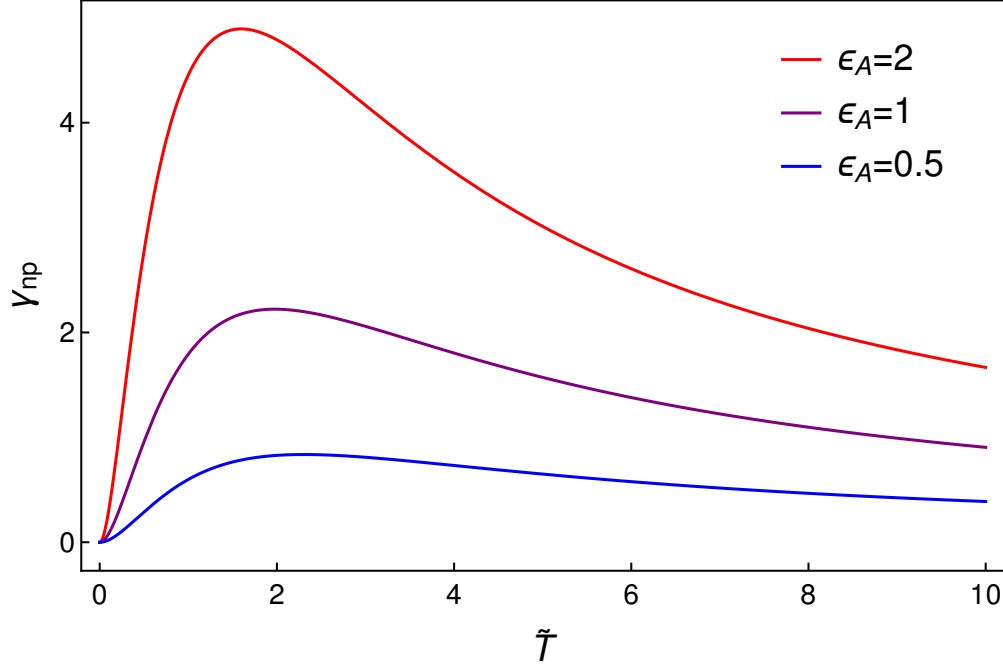


Figure 6. $\sigma_{PC}(t)$ +Gaussian white noise: non-Gaussian parameter (γ_{np}) is plotted as a function of scaled time \tilde{T} for three different values of ϵ_A , keeping $\tilde{\tau}(= \tau_a/\tau_p)$ fixed at 20. The features of the plots remain unaltered for any particular ratio of τ_p and τ_a .

the dynamics can be investigated by finding PDF. To do that we have to invert $\mathbb{F}(p_T)$ to the position space as shown in Eq. (54). But as the inverse Fourier transform cannot be done analytically, one needs to do it numerically. However, one can get the asymptotic behaviors of the PDF. Before proceeding further we rescale x_f , p_T by a_0 , introducing $\tilde{x}_f = \frac{x_f}{a_0}$, $\tilde{p}_T = a_0 p_T$. Eq. (54) can be rewritten in terms of these as

$$\mathbb{P}(\tilde{x}_f, \tilde{T}; \tilde{x}_0 = 0, 0) = \frac{1}{2\pi} \int_{-\infty}^{+\infty} d\tilde{p}_T e^{-i\tilde{p}_T \tilde{x}_f} \mathbb{F}(\tilde{p}_T), \quad (58)$$

where

$$\mathbb{F}(\tilde{p}_T) = e^{-\frac{\tilde{T} \tilde{p}_T^2}{\tilde{\tau} \epsilon_A}} \exp \left[-\frac{1}{\tilde{\tau}} \frac{\tilde{p}_T}{1 + \tilde{p}_T^2} \left(\tilde{T} \tilde{p}_T - \tan^{-1}(\rho \tilde{p}_T) \right) \right] (1 + \rho^2 \tilde{p}_T^2)^{-\frac{1}{2\tilde{\tau}} \frac{\tilde{p}_T^2}{1 + \tilde{p}_T^2}}. \quad (59)$$

We now consider different limits, which can be looked at analytically.

1. $\tilde{T} \ll 1$ and \tilde{x}_f arbitrary.

In the short time limit,

$$\exp \left[-\frac{1}{\tilde{\tau}} \frac{\tilde{p}_T}{1 + \tilde{p}_T^2} \left(\tilde{T} \tilde{p}_T - \tan^{-1}(\rho \tilde{p}_T) \right) \right] \approx 1, \quad (60)$$

so that

$$\mathbb{F}(\tilde{p}_T) \approx e^{-\frac{\tilde{T}}{\tilde{\tau}} \frac{\tilde{p}_T^2}{\epsilon_A}} (1 + \rho^2 \tilde{p}_T^2)^{-\frac{1}{2\tilde{\tau}} \frac{\tilde{p}_T^2}{1 + \tilde{p}_T^2}}. \quad (61)$$

So the probability distribution function is the convolution of a Gaussian, of width $\sim \sqrt{\tilde{T}/(\tilde{\tau}\epsilon_A)}$ with the inverse Fourier transform of the function $(1 + \rho^2 \tilde{p}_T^2)^{-\frac{1}{2\tilde{\tau}} \frac{\tilde{p}_T^2}{1 + \tilde{p}_T^2}}$, which we will denote as $h(\tilde{x}_f)$. Though the inverse Fourier transform cannot be done analytically, the width of the resulting function can be estimated to be $\sim \rho \approx \tilde{T}$. As $\tilde{T} \ll 1$, if one has $\sqrt{\tilde{T}/(\tilde{\tau}\epsilon_A)} \gg \tilde{T}$ then $h(\tilde{x}_f)$ can be approximated as a Dirac delta function. Hence in this limit

$$\mathbb{P}(\tilde{x}_f, \tilde{T}; \tilde{x}_0 = 0, 0) = \sqrt{\frac{\epsilon_A \tilde{\tau}}{4\pi \tilde{T}}} \exp \left(-\frac{\epsilon_A \tilde{\tau} \tilde{x}_f^2}{4\tilde{T}} \right). \quad (62)$$

Thus the distribution displays predominant signature of white noise.

2. Long time ($\tilde{T} \gg 1$), large \tilde{x}_f ($\tilde{x}_f \gg 1$) limit.

At large displacement (*i.e.* $x_f \gg a_0$, or equivalently $\tilde{p}_T \ll 1$) and for long time ($\tilde{T} \gg 1$, $\Rightarrow \rho \approx 1$) limit one can express $\mathbb{F}(\tilde{p}_T)$ as a Gaussian function of \tilde{p}_T , *viz.*,

$$\mathbb{F}(\tilde{p}_T) \approx e^{-\frac{\tilde{T}}{\tilde{\tau}} \left(1 + \frac{1}{\epsilon_A}\right) \tilde{p}_T^2}. \quad (63)$$

Hence the PDF can be easily obtained by Fourier inversion of Eq. (63) and it is given as

$$\mathbb{P}(\tilde{x}_f, \tilde{T}; \tilde{x}_0 = 0, 0) = \sqrt{\frac{\tilde{\tau} \epsilon_A}{4(1 + \epsilon_A) \pi \tilde{T}}} e^{-\frac{\epsilon_A}{1 + \epsilon_A} \frac{\tilde{\tau} \tilde{x}_f^2}{4\tilde{T}}}. \quad (64)$$

So, in this limit the particle is Gaussian-distributed with a total diffusivity of $D + D_A$.

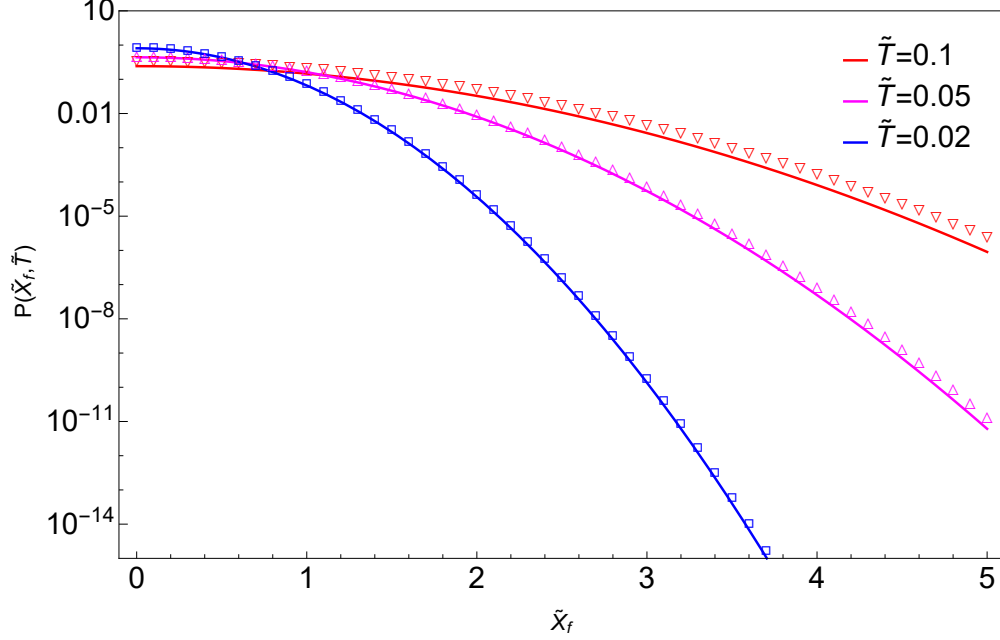


Figure 7. Probability distribution function, plotted as a function of the scaled displacement in logarithmic scale for different values of time. The plots are for the values of parameters: $\{\tilde{\tau} = 0.2, \epsilon_A = 1\}$. The plots with symbols are obtained after numerical integration of Eq. (58) and solid curves represent Eq. (62).

3. Different time limits, but small \tilde{x}_f

In this case, $\tilde{x}_f \ll 1$. This implies $\tilde{p}_T \gg 1$, and the terms in Eq. (61) can be approximated as follows:

$$\exp\left[-\frac{1}{\tilde{\tau}} \frac{\tilde{p}_T}{1 + \tilde{p}_T^2} \left(\tilde{T} \tilde{p}_T - \tan^{-1}(\rho \tilde{p}_T)\right)\right] \approx \exp\left[-\frac{\tilde{T}}{\tilde{\tau}} + \frac{\tilde{T}}{\tilde{p}_T} \tan^{-1}(\rho \tilde{p}_T)\right] \approx e^{-\frac{\tilde{T}}{\tilde{\tau}}},$$

and

$$(1 + \rho^2 \tilde{p}_T^2)^{-\frac{1}{2\tilde{\tau}}} \frac{\tilde{p}_T^2}{1 + \tilde{p}_T^2} \approx (1 + \rho^2 \tilde{p}_T^2)^{-\frac{1}{2\tilde{\tau}}}. \quad (65)$$

Therefore, distribution of displacement as given in Eq. (58) can be approximated as

$$\mathbb{P}(\tilde{x}_f, \tilde{T}; \tilde{x}_0 = 0, 0) \approx \frac{e^{-\frac{\tilde{T}}{\tilde{\tau}}}}{2\pi} \int_{-\infty}^{+\infty} d\tilde{p}_T e^{-i\tilde{p}_T \tilde{x}_f} \frac{e^{-\frac{\tilde{T}}{\tilde{\tau}} \frac{\tilde{p}_T^2}{\epsilon_A}}}{(1 + \rho^2 \tilde{p}_T^2)^{\frac{1}{2\tilde{\tau}}}}. \quad (66)$$

The above can be rewritten as a convolution of two functions as outlined in section III C

and it reads

$$\mathbb{P}(\tilde{x}_f, \tilde{T}; \tilde{x}_0 = 0, 0) = \int_{-\infty}^{+\infty} d\tilde{x} \sqrt{\frac{\epsilon_A \tilde{T}}{4\pi \tilde{T}}} e^{-\frac{\tilde{T}}{\tilde{\tau}} - \epsilon_A \tilde{\tau} (\tilde{x}_f - \tilde{x})^2 / (4\tilde{T})} \frac{2^{\frac{3}{2} - \frac{1}{2\tilde{\tau}}} \sqrt{\pi} \left| \frac{\tilde{x}}{\rho} \right|^{\frac{1}{2\tilde{\tau}} - \frac{1}{2}} K_{\frac{1}{2\tilde{\tau}} - \frac{1}{2}} \left(\frac{|\tilde{x}|}{\rho} \right)}{\Gamma\left(\frac{1}{2\tilde{\tau}}\right)}. \quad (67)$$

The above integration cannot be done analytically. So we analyze limiting situations in the following. In the limit where such analysis is not possible, we evaluate the integral numerically. Our numerical results match these analytical results, and also interpolate between these limits.

The Gaussian, due to thermal noise has the width $\sqrt{\frac{2\tilde{T}}{\epsilon_A \tilde{\tau}}}$ and the Bessel function has the width ρ . If the Gaussian has negligible width compared to that of Bessel function, *i.e.*, if $\frac{\epsilon_A \tilde{\tau} \rho^2}{2\tilde{T}} \gg \rho \approx 1$, then the Gaussian can be approximated as a delta function, and the integration performed. The result is

$$\mathbb{P}(\tilde{x}_f, \tilde{T}) \approx \frac{2^{\frac{3}{2} - \frac{1}{2\tilde{\tau}}} \sqrt{\pi}}{\Gamma\left(\frac{1}{2\tilde{\tau}}\right)} \left| \frac{\tilde{x}_f}{\rho} \right|^{\frac{1}{2\tilde{\tau}} - \frac{1}{2}} K_{\frac{1}{2\tilde{\tau}} - \frac{1}{2}} \left(\frac{|\tilde{x}_f|}{\rho} \right). \quad (68)$$

On the other hand, in the limit $\sqrt{\frac{2\tilde{T}}{\epsilon_A \tilde{\tau}}} \gg \rho$ or for $1 \gg \frac{\epsilon_A \tilde{\tau} \rho^2}{2\tilde{T}}$, Bessel function can be approximated by a Dirac delta function and one gets

$$\mathbb{P}(\tilde{x}_f, \tilde{T}; \tilde{x}_0 = 0, 0) \approx e^{-\frac{\tilde{T}}{\tilde{\tau}}} \sqrt{\frac{\epsilon_A \tilde{T}}{4\pi \tilde{T}}} e^{-\frac{\epsilon_A \tilde{\tau}}{4\tilde{T}} \tilde{x}_f^2}. \quad (69)$$

Another approximation, which requires $\rho \tilde{p}_T \gg 1$ and $\tilde{p}_T \gg 1$ is given below. In this case,

$$\mathbb{F}(\tilde{p}_T) \approx \frac{e^{-\frac{\tilde{T}}{\tilde{\tau}}}}{2\pi} \int_{-\infty}^{+\infty} d\tilde{p}_T e^{-i\tilde{p}_T \tilde{x}_f} \frac{e^{-\frac{\tilde{T}}{\tilde{\tau}} \frac{\tilde{p}_T^2}{\epsilon_A}}}{(1 + \rho^2 \tilde{p}_T^2)^{\frac{1}{2\tilde{\tau}}}},$$

which may be approximated as

$$\mathbb{P}(\tilde{x}_f, \tilde{T}; \tilde{x}_0 = 0, 0) \approx \frac{e^{-\frac{\tilde{T}}{\tilde{\tau}}}}{2\pi} \int_{-\infty}^{+\infty} d\tilde{p}_T e^{-i\tilde{p}_T \tilde{x}_f} \frac{e^{-\frac{\tilde{T}}{\tilde{\tau}} \frac{\tilde{p}_T^2}{\epsilon_A}}}{(\rho^2 \tilde{p}_T^2)^{\frac{1}{2\tilde{\tau}}}}. \quad (70)$$

For $\tilde{\tau} > 1$, the above can be done analytically and leads to

$$\mathbb{P}(\tilde{x}_f) = \frac{\Gamma\left(\frac{1}{2} - \frac{1}{2\tilde{\tau}}\right)}{2\pi} e^{-\frac{\tilde{T}}{\tilde{\tau}}} \rho^{-\frac{1}{\tilde{\tau}}} \left(\frac{\tilde{T}}{\tilde{\tau} \epsilon_A} \right)^{-\frac{1}{2}(1 - \frac{1}{\tilde{\tau}})} {}_1F_1 \left(\frac{1}{2} - \frac{1}{2\tilde{\tau}}; \frac{1}{2}; -\epsilon_A \frac{\tilde{x}_f^2 \tilde{\tau}}{4\tilde{T}} \right), \quad (71)$$

where ${}_1F_1(a, b; z)$ is Kummer confluent hypergeometric function of first kind [51]. The function in Eq. (71) has a central Gaussian core like Eq. (69), and deviates from it as may be seen in the insets of Fig. 9.

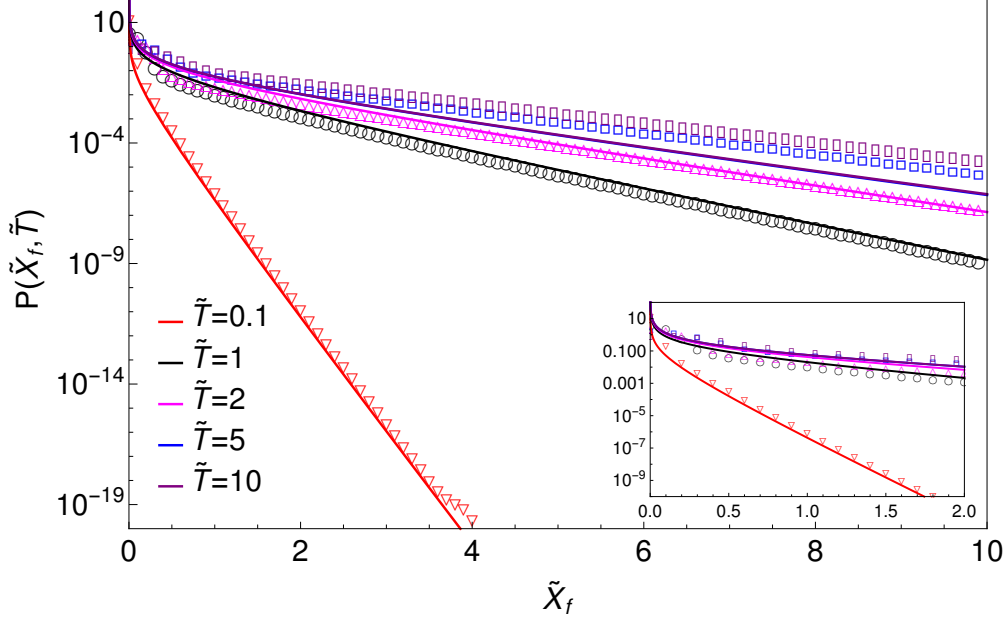


Figure 8. Logarithmic values of probability distribution function is plotted against scaled displacement for different values of time keeping parameters fixed at $\tilde{\tau} = 20$, $\epsilon_A = 10$. The plots with symbols is obtained from Eq. (58) after numerical integration and solid curves represent Eq. (68). The same plots have been enlarged in the inset to obtain behavior near origin.

We have performed the numerical integration of Eq. (58) and made plots at different times for the same normal and active diffusivities, as shown in Fig. 7- 9. Fig. 7 demonstrates the behavior of distribution in the limit $1 \gg \frac{\epsilon_A \tilde{\tau} \rho^2}{2\tilde{T}}$ at small position and suggests Gaussian distribution of the form given in Eq. (62). Fig. 9 is drawn in the following regime : $\frac{\tilde{T}}{\tilde{\tau}} \ll 1$, $\tilde{\tau} > 1$ and $\epsilon_A \sim \mathcal{O}(1)$. In the inset, numerical values show that at small \tilde{x}_f , the distribution is Gaussian, but at higher values it deviates. The deviation from Gaussianity is described by Eq. (68). For the system with higher active diffusivity, the central Gaussian shape has virtually zero width. Hence, throughout entire position range it basically follows the same distribution (68) as shown in Fig. 8.

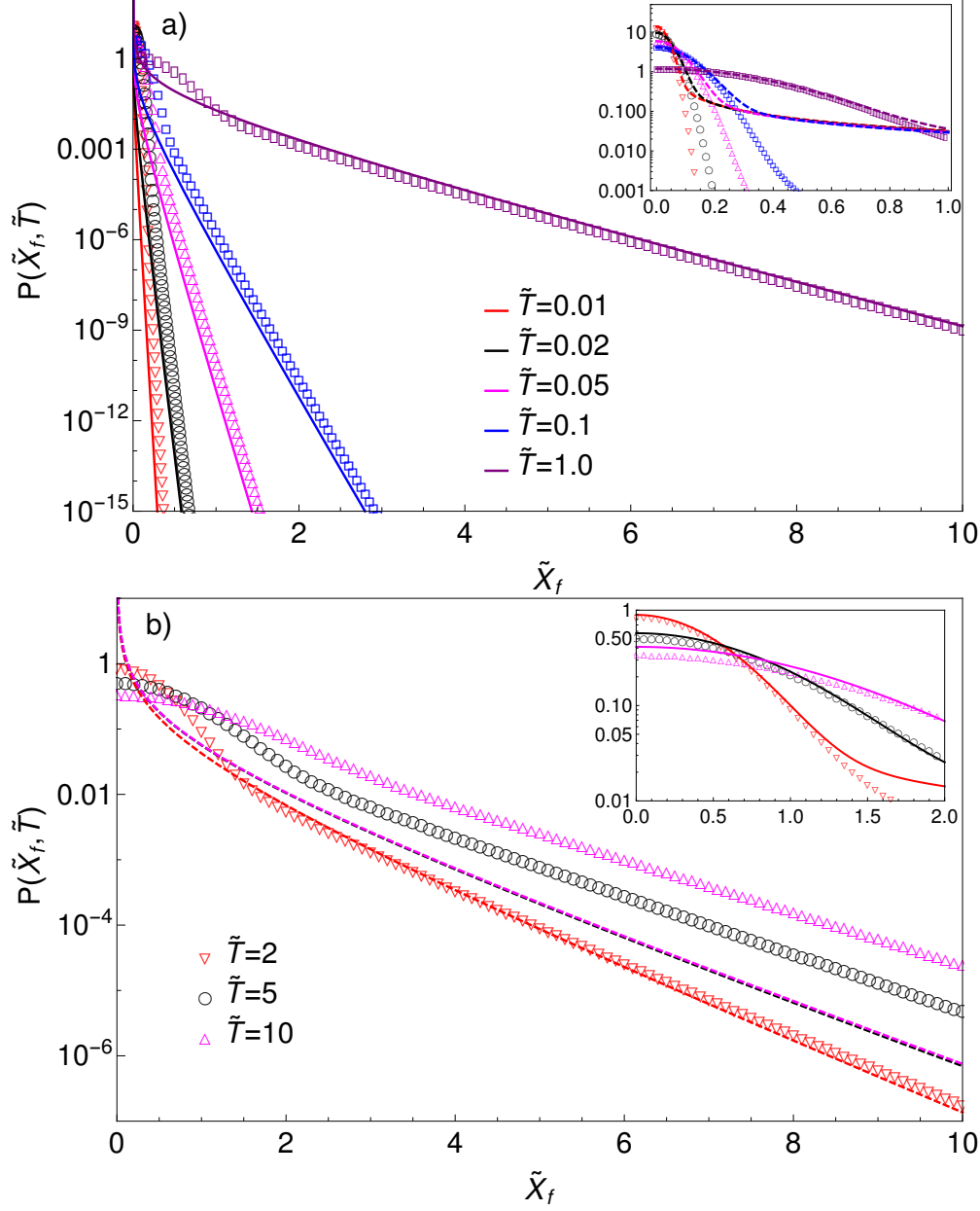


Figure 9. The Logarithmic plot of probability distribution function vs. displacement at intermediate time scale for (a) $\tilde{T} \ll \tilde{\tau}$ and (b) $\tilde{T} < \tilde{\tau}$, where $\tilde{\tau} > 1$. All the curves with symbols have been obtained from numerical integration of Eq. (58) taking $\epsilon_A = 1$ and $\tilde{\tau} = 20$. In Fig. a, Eq. (68) are drawn as solid curves for entire position range at different times, which agree well with the numerical results at positions away from origin. Near the origin, the result agrees well with Eq. (71) corresponding to dashed curves as shown in the inset. In the inset of b), solid curves correspond to Eq. (71) for different times which are quite a good fit. The results in b) are for longer times. The curves are obtained using Eq. (68) and are seen to be in poor agreement with numerical results.

IV. RESULTS FOR HARMONIC OSCILLATOR IN DIFFERENT TYPES OF NOISES $\sigma(t)$

A. Gaussian colored Noise

Consider $\sigma(t)$ as colored Gaussian noise and the particle is initially at an equilibrium distribution of the form: $P(x_0) = \sqrt{\frac{\lambda}{2\pi D}} e^{-\frac{\lambda}{2D} x_0^2}$. The characteristic function $\mathbb{G}(p_T)$ in Eq. (13) can be computed using Eq. (15) and it is given as

$$\mathbb{G}(p_T) = \exp \left[-\frac{D_A p_T^2}{2\lambda(\lambda^2 \tau^2 - 1)} \left((\lambda\tau - 1) - 2\lambda\tau e^{-T(\lambda+1/\tau)} + (\lambda\tau + 1)e^{-2T\lambda} \right) \right]. \quad (72)$$

Therefore the Fourier transform of probability distribution function, $\mathbb{F}(p_T)$ can be written as

$$\mathbb{F}(p_T) = \exp \left[-\frac{D_A p_T^2}{2\lambda(\lambda^2 \tau^2 - 1)} \left((\lambda\tau - 1) - 2\lambda\tau e^{-T(\lambda+1/\tau)} + (\lambda\tau + 1)e^{-2T\lambda} \right) - \frac{D p_T^2}{2\lambda} \right]. \quad (73)$$

Using Eq. (22) one can obtain MSD which is given as

$$\langle x(T)^2 \rangle = \frac{D_A}{\lambda(\lambda^2 \tau^2 - 1)} \left((\lambda\tau - 1) - 2\lambda\tau e^{-T(\lambda+1/\tau)} + (\lambda\tau + 1)e^{-2T\lambda} \right) + \frac{D}{\lambda}. \quad (74)$$

At short time limit $\langle x(T)^2 \rangle = D/\lambda$, which is the MSD at equilibrium distribution. But with the passage of time, $\sigma(t)$ comes into effect as it is evident from the value of MSD, which is given for very large time limit as: $\langle x(T)^2 \rangle = \frac{1}{\lambda} \left[D + \frac{D_A}{1+\lambda\tau} \right]$.

As $\mathbb{F}(p_T)$ is Gaussian, its Fourier transform is easily computed to get

$$\mathbb{P}(x_f, T) = \sqrt{\frac{1}{2\pi\theta^2}} e^{-\frac{x_f^2}{2\theta^2}}, \quad (75)$$

where $\theta^2 = \langle x(T)^2 \rangle$. Therefore the particle is Gaussian distributed at all times, with a width which has contribution from both D and D_A . At large time limit the width of the distribution becomes time independent as obvious with a value $\frac{1}{\lambda} \left[D + \frac{D_A}{1+\lambda\tau} \right]$.

B. Dichotomous Poisson Noise

We consider here the case where the dynamics of a particle (*e.g.*, Janus particles or flagellated bacteria) is driven by both white Gaussian and dichotomous noise, in a harmonic

potential $V(x) = \frac{\lambda x^2}{2}$. The dichotomous noise has mean zero and an exponential correlation, *viz.*,

$$\begin{aligned}\langle \sigma_{DP}(t) \rangle &= 0 \\ \langle \sigma_{DP}(t) \sigma_{DP}(t') \rangle &= u^2 e^{-\gamma|t-t'|} = D_A \gamma e^{-\gamma|t-t'|}.\end{aligned}\quad (76)$$

Here, diffusivity in active noise D_A is defined as: $D_A = \frac{u^2}{\gamma}$. The noise $\sigma(t)$ can be described by the characteristic function defined by [46]

$$\begin{aligned}G(p_T) &= \left\langle e^{ip_T e^{-\lambda T} \int_0^T dt e^{\lambda t} \sigma_{DP}(t)} \right\rangle = {}_0F_1 \left(\frac{\alpha+1}{2}, -\frac{p_T^2 u^2}{4\lambda^2} \right) {}_0F_1 \left(\frac{-\alpha+1}{2}, -\frac{p_T^2 u^2}{4\lambda^2} e^{-2\lambda T} \right) \\ &+ \frac{u^2 p_T^2 e^{-(\gamma+\lambda)T}}{\lambda^2(\alpha+1)(-\alpha+1)} {}_0F_1 \left(\frac{-\alpha+3}{2}, -\frac{p_T^2 u^2}{4\lambda^2} \right) {}_0F_1 \left(\frac{\alpha+3}{2}, -\frac{p_T^2 u^2}{4\lambda^2} e^{-2\lambda T} \right),\end{aligned}\quad (77)$$

where $\alpha = \frac{\gamma}{\lambda}$, which is the signature of the active noise. Considering the particle to be initially in the equilibrium state which would result in the absence of active noise σ_{DP} , the probability distribution function that would result at T may be written as

$$\mathbb{P}(x_f, T) = \frac{1}{2\pi} \int_{-\infty}^{+\infty} dp_T e^{-ip_T x_f} e^{-\frac{D}{2\lambda} p_T^2} G(p_T).\quad (78)$$

It should be noted that the final steady state form of the distribution would be independent of the initial starting distribution. Now let us define dimensionless variables as: $\tilde{x}_f = x_f \frac{\gamma}{u}$, $\tilde{p}_T = p_T \frac{u}{\gamma}$, $\tilde{T} = \lambda T$, $\epsilon_A = \frac{D_A}{D}$. Then, Eq. (78) can be rewritten as

$$\mathbb{P}(\tilde{x}_f, \tilde{T}) = \frac{1}{2\pi} \int_{-\infty}^{+\infty} d\tilde{p}_T e^{-i\tilde{p}_T \tilde{x}_f} e^{-\frac{\alpha}{2\epsilon_A} \tilde{p}_T^2} G(\tilde{p}_T),\quad (79)$$

with

$$\begin{aligned}G(\tilde{p}_T) &= {}_0F_1 \left(\frac{\alpha+1}{2}, -\frac{\tilde{p}_T^2 \alpha^2}{4} \right) {}_0F_1 \left(\frac{-\alpha+1}{2}, -\frac{\tilde{p}_T^2 \alpha^2}{4} e^{-2\tilde{T}} \right) \\ &+ \frac{\tilde{p}_T^2 \alpha^2 e^{-(\alpha+1)\tilde{T}}}{(\alpha+1)(-\alpha+1)} {}_0F_1 \left(\frac{-\alpha+3}{2}, -\frac{\tilde{p}_T^2 \alpha^2}{4} \right) {}_0F_1 \left(\frac{\alpha+3}{2}, -\frac{\tilde{p}_T^2 \alpha^2}{4} e^{-2\tilde{T}} \right).\end{aligned}\quad (80)$$

The MSD of the distribution at time \tilde{T} is

$$\langle \tilde{x}^2(\tilde{T}) \rangle = \frac{\alpha^2}{1+\alpha} - \frac{2\alpha^2}{1-\alpha^2} e^{-(1+\alpha)\tilde{T}} + \frac{\alpha^2}{1-\alpha} e^{-2\tilde{T}} + \frac{\alpha}{\epsilon_A}.\quad (81)$$

At short time, $\langle \tilde{x}^2(\tilde{T}) \rangle \sim \frac{\alpha}{\epsilon_A}$ suggesting as appropriate for the initial equilibrium state. Notice that $\langle \tilde{x}^2(\tilde{T}) \rangle \rightarrow 0$ if $\epsilon_A \rightarrow \infty$, reflecting the fact that initial contribution comes from

white noise. After a long time, $\langle \tilde{x}^2(\tilde{T}) \rangle \sim \frac{\alpha^2}{1+\alpha} + \frac{\alpha}{\epsilon_A}$, which includes the effect of active noise. By virtue of Eq. (22) and Eq. (79), fourth moment is calculated at $\tilde{T} \rightarrow \infty$ limit and it is given by

$$\langle \tilde{x}^4(\tilde{T}) \rangle = \frac{3\alpha^4}{2(\alpha+1)\left(\frac{\alpha+1}{2}+1\right)} + \frac{6\alpha^3}{(\alpha+1)\epsilon_A} + \frac{3\alpha^2}{\epsilon_A^2}. \quad (82)$$

Subsequently, using Eq. (24) NGP is computed in this limit and it reads

$$\gamma_{np} = - \left(\frac{2}{3+\alpha} \right) \left(\frac{1}{1 + \frac{1}{\epsilon_A} + \frac{1}{\alpha\epsilon_A}} \right)^2. \quad (83)$$

For the limit $\alpha \rightarrow \infty$, γ_{np} diminishes to zero, which corresponds to a Gaussian distribution. At the limit $\alpha \rightarrow 0$, $\gamma_{np} = -\frac{2}{3} \left(\frac{1}{1 + \frac{1}{\epsilon_A} + \frac{1}{\alpha\epsilon_A}} \right)^2$, which is always negative. Notice that, for finite stiffness the term $\alpha\epsilon_A$ must be non-zero even at $\alpha \rightarrow 0$ limit if the active noise is operating on, as this term determines its strength of correlation. For any other values of α , γ_{np} takes negative value with a minimum occurring at $\alpha = \frac{1}{2} \frac{1 + \sqrt{25 + 24\epsilon_A}}{1 + \epsilon_A}$, indicating the distribution decays faster than Gaussian. For any finite value of α , γ_{np} is monotonically decreasing function with respect to ϵ_A , starting with $\gamma_{np} = 0$ at the limit $\epsilon_A \rightarrow 0$. It suggests, for small diffusivity of active noise the distribution becomes Gaussian centered at $\tilde{x}_f = 0$ as shown in Fig. 10.

To get an entire description of the dynamics, we need to perform the Fourier inversion as given in Eq. (79) which is difficult to do. However, at the long time limit $\tilde{T} \rightarrow \infty$, the characteristic function can be simplified to

$$\mathcal{L}t_{T \rightarrow \infty} G(\tilde{p}_T) = G_0(\tilde{p}_T) = {}_0F_1 \left(\frac{\alpha+1}{2}, -\frac{\tilde{p}_T^2 \alpha^2}{4} \right). \quad (84)$$

Therefore the distribution takes a simple form as

$$\mathbb{P}_{st}(\tilde{x}_f) = \frac{1}{2\pi} \int_{-\infty}^{+\infty} d\tilde{p}_T e^{-i\tilde{p}_T \tilde{x}_f} e^{-\frac{\alpha}{2\epsilon_A} \tilde{p}_T^2} G_0(\tilde{p}_T). \quad (85)$$

Along with Gaussian Fourier transform $\frac{1}{2\pi} \int_{-\infty}^{+\infty} d\tilde{p}_T e^{-i\tilde{p}_T \tilde{x}_f} e^{-\frac{\alpha}{2\epsilon_A} \tilde{p}_T^2} = \sqrt{\frac{\epsilon_A}{2\pi\alpha}} e^{-\frac{\epsilon_A}{2\alpha} \tilde{x}_f^2}$, the following transform is required for calculation of $\mathbb{P}_{st}(x_f)$:

$$\int_{-\infty}^{+\infty} d\tilde{p}_T e^{-i\tilde{p}_T \tilde{x}} G_0(\tilde{p}_T) = \frac{\Gamma(\frac{\alpha+1}{2})}{\sqrt{\pi}\Gamma(\frac{\alpha}{2})} \frac{1}{\alpha} \left(1 - \frac{\tilde{x}^2}{\alpha^2} \right)^{\alpha/2-1} \left(1 - \Theta\left(1 - \frac{\alpha^2}{\tilde{x}^2}\right) \right). \quad (86)$$

Hence, the steady state probability can be rewritten as convolution of the above two Fourier transforms as

$$\mathbb{P}_{st}(\tilde{x}_f) = \frac{\Gamma(\frac{\alpha+1}{2})}{\sqrt{\pi}\Gamma(\frac{\alpha}{2})} \frac{1}{\alpha} \sqrt{\frac{\epsilon_A}{2\pi\alpha}} \int_{-\alpha}^{+\alpha} d\tilde{y} e^{-\frac{\epsilon_A}{2\alpha} (\tilde{x}_f - \tilde{y})^2} \left(1 - \frac{\tilde{y}^2}{\alpha^2} \right)^{\alpha/2-1}. \quad (87)$$

We need to compute Eq. (87) which is not possible analytically. However one can consider the following limiting cases, for which the analysis can be carried out.

1. $\epsilon_A \gg 1$.

This limit corresponds to a situation where the width of Gaussian, α/ϵ_A is much smaller than α which is the width of other function involved in the convolution with Gaussian in Eq. (87). Hence,

$$\sqrt{\frac{\epsilon_A}{2\pi\alpha}} e^{-\frac{\epsilon_A}{2\alpha}(\tilde{x}_f - \tilde{y})^2} \approx \delta(\tilde{x}_f - \tilde{y}).$$

Therefore, the steady state distribution becomes

$$\mathbb{P}_{st}(\tilde{x}_f) = \frac{\Gamma(\frac{\alpha+1}{2})}{\sqrt{\pi}\Gamma(\frac{\alpha}{2})} \frac{1}{\alpha} \left(1 - \frac{\tilde{x}_f^2}{\alpha^2}\right)^{\alpha/2-1}. \quad (88)$$

This result had been reported for non-interacting run-and-tumble particles confined within a circular pore [38, 52]. Here, the effect of thermal noise is negligible compared to active noise and as a consequence the distribution remains confined in the region $[-\alpha, +\alpha]$.

2. $\epsilon_A \ll 1$.

In this case, normal diffusivity prevails over the active one. Taking $\alpha \ll \frac{\alpha}{\epsilon_A}$ or $\epsilon_A \ll 1$, one can approximate $\frac{\Gamma(\frac{\alpha+1}{2})}{\sqrt{\pi}\Gamma(\frac{\alpha}{2})} \frac{1}{\alpha} \left(1 - \frac{\tilde{x}_f^2}{\alpha^2}\right)^{\alpha/2-1} \approx \delta(\tilde{x}_f)$ to get

$$\mathbb{P}_{st}(\tilde{x}_f) = \sqrt{\frac{\epsilon_A}{2\pi\alpha}} e^{-\frac{\epsilon_A}{2\alpha}\tilde{x}_f^2}. \quad (89)$$

Therefore for small value of ϵ_A , distribution is Gaussian with a long spread, centered at $\tilde{x}_f = 0$, as pictorially depicted in Fig. 10.

3. $\alpha \gg 1$.

The Fourier transform of $G_0(\tilde{p}_T)$ given in Eq. (86) can be approximated at large α limit as given below.

According to Stirling's approximation, for large β , $\Gamma(\beta) \approx \sqrt{\frac{2\pi}{\beta}} \left(\frac{\beta}{e}\right)^\beta (1 + \mathcal{O}(1/\beta))$. Using this, for $\alpha \gg 1$, one can approximate $\frac{\Gamma(\frac{\alpha+1}{2})}{\Gamma(\frac{\alpha}{2})} \approx \sqrt{\frac{\alpha}{2}}$ and $(1 + \frac{1}{\alpha})^{\frac{\alpha}{2}} \approx \sqrt{e}$. Further,

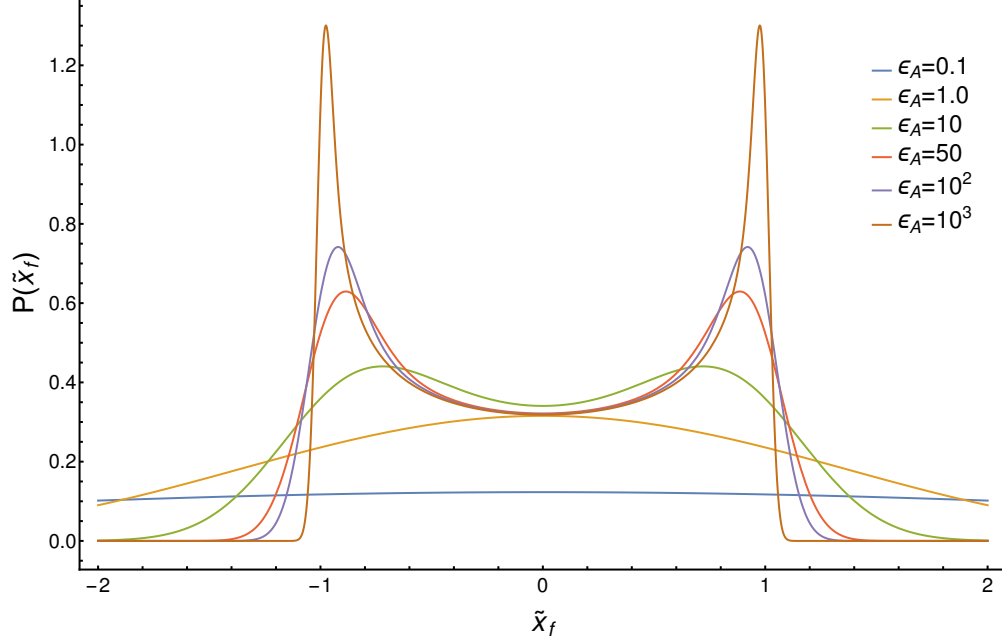


Figure 10. Steady state distribution of particle confined in a harmonic potential in dichotomous noise is plotted against displacement for different values of ϵ_A at $\alpha = 1$.

$\left(1 - \frac{\tilde{y}^2}{\alpha^2}\right)^{\alpha/2-1} \simeq e^{\ln\left(1 - \frac{\tilde{y}^2}{\alpha^2}\right)\alpha/2} \simeq e^{-\frac{\tilde{y}^2}{2\alpha} - \mathcal{O}\left(\frac{1}{\alpha^3}\right)} \sim e^{-\frac{\tilde{y}^2}{2\alpha}}$. Therefore at very large α limit the probability distribution from Eq. (87) can be written as

$$\mathbb{P}_{st}(\tilde{x}_f) = \sqrt{\frac{1}{2\pi\alpha}} \sqrt{\frac{\epsilon_A}{2\pi\alpha}} \int_{-\infty}^{+\infty} d\tilde{y} e^{-\frac{\epsilon_A}{2\alpha}(\tilde{x}_f - \tilde{y})^2} e^{-\frac{\tilde{y}^2}{2\alpha}} = \sqrt{\frac{1}{2\pi\alpha\left(1 + \frac{1}{\epsilon_A}\right)}} e^{-\frac{\tilde{x}_f^2}{2\pi\alpha\left(1 + \frac{1}{\epsilon_A}\right)}}. \quad (90)$$

For finite stiffness of potential, large α regime reflects large γ , which becomes delta correlated at this limit. As a consequence the steady state distribution is Gaussian as given in Eq. (90).

4. $\alpha \ll 1$.

At very small α limit, one can write: $\frac{\Gamma(\frac{\alpha+1}{2})}{\Gamma(\frac{\alpha}{2})} \approx \frac{\alpha\sqrt{\pi}}{2}$. The other term in $G_0(\tilde{p}_T)$ can be approximated as

$$\left(1 - \frac{\tilde{y}^2}{\alpha^2}\right)^{\alpha/2-1} \approx e^{-\ln\left(1 - \frac{\tilde{y}^2}{\alpha^2}\right)} \approx \delta(\tilde{y} - \alpha) + \delta(\tilde{y} + \alpha). \quad (91)$$

Therefore by virtue of Eq. (86) and Eq. (91), Eq. (87) can be computed as

$$\mathbb{P}_{st}(\tilde{x}_f) = \frac{1}{2} \sqrt{\frac{\epsilon_A}{2\pi\alpha}} \left[e^{-\frac{\epsilon_A}{2\alpha}(\tilde{x}_f - \alpha)^2} + e^{-\frac{\epsilon_A}{2\alpha}(\tilde{x}_f + \alpha)^2} \right] \approx \frac{1}{2} \delta(\tilde{x}_f - \alpha) + \frac{1}{2} \delta(\tilde{x}_f + \alpha). \quad (92)$$

Small α implies the very slow Poisson rate. Hence one should expect particle to be gathered almost deterministically at two positions $+\alpha$, $-\alpha$. The analytical approximate result given in Eq. (92) as well as the plot in Fig. 11 support this statement.

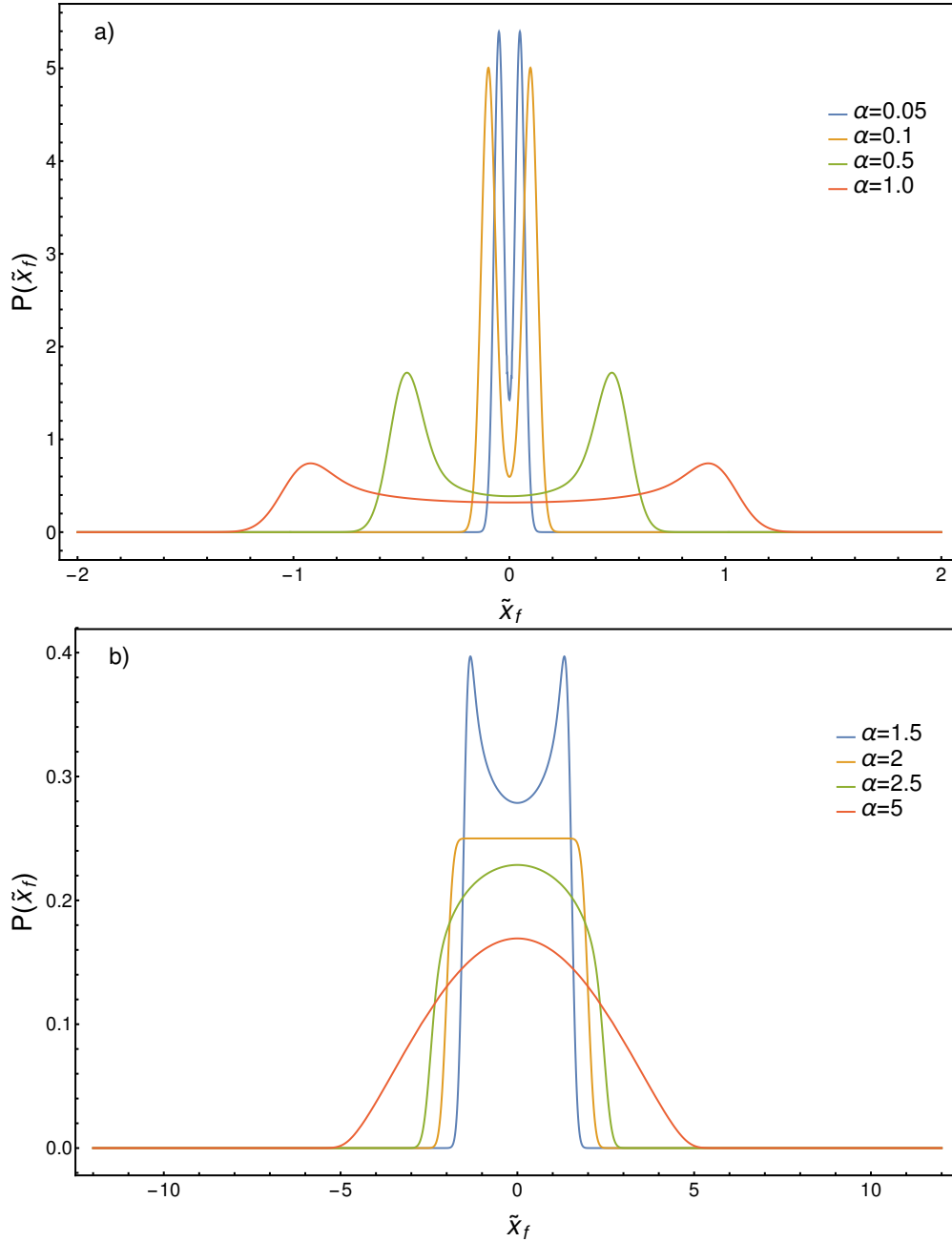


Figure 11. Steady state distribution of a confined particle in presence of dichotomous noise is plotted against scaled displacement for different values of α at $\epsilon_A = 100$.

5. $\alpha = 2$.

For $\alpha = 2$, the integration involving in Eq. (87) can be evaluated exactly which results

$$\mathbb{P}_{st}(\tilde{x}_f) = \frac{1}{4\alpha} \left[\operatorname{erf} \left(\sqrt{\frac{\epsilon_A}{2\alpha}} [\tilde{x}_f + \alpha] \right) - \operatorname{erf} \left(\sqrt{\frac{\epsilon_A}{2\alpha}} [\tilde{x}_f - \alpha] \right) \right]. \quad (93)$$

Notice that the distribution at $\alpha = 2$ is almost flat, whereas for $\alpha < 2$ the distribution is bimodal and for $\alpha > 2$ it is single peaked as illustrated in Fig. 11. Therefore $\alpha = 2$ represents a crossover regime. It is interesting to note here that similar trait has been observed for a model with switching environments where alteration of switching rate from slow to fast transits the distribution from bimodal to unimodal [53].

C. Poissonian White Noise

Here we consider a particle undergoing random walk in a harmonic potential in presence of both Gaussian white noise $\eta(t)$ and Poissonian white noise $\sigma_{PW}(t)$. The particle is initially Gaussian distributed with a distribution: $P(x_0) = \sqrt{\frac{\lambda}{2\pi D}} e^{-\frac{\lambda}{2D} x_0^2}$. Using Eq. (35) we have calculated characteristic functional which is given as

$$\mathbb{G}(p_T) = \left[\frac{1 + a_0^2 p_T^2 e^{-2\lambda T}}{1 + a_0^2 p_T^2} \right]^{\frac{\mu}{2\lambda}}. \quad (94)$$

Therefore from Eq. (12) one can express the propagator as

$$\mathbb{P}(x_f, T; x_0, 0) = \frac{1}{2\pi} \int_{-\infty}^{+\infty} dp_T e^{-ip_T x_f + ip_0 x_0 - \frac{D p_T^2}{2\lambda} (1 - e^{-2\lambda T})} \mathbb{G}(p_T). \quad (95)$$

The relaxation time of the particle in the harmonic potential is denoted here as τ_r and is given by: $\tau_r = \frac{1}{\lambda}$. The characteristic timescale to occur a Poisson pulse is defined as: $\tau_a = \frac{1}{\mu}$. So we can write down a dimensionless parameter $\tilde{\tau}$ as $\tilde{\tau} = \frac{\tau_a}{\tau_r}$. Using Eq. (95) into Eq. (14) one can obtain the probability of finding the particle at position x_f at time T and it reads

$$\mathbb{P}(x_f, T) = \frac{1}{2\pi} \int_{-\infty}^{+\infty} dp_T e^{-ip_T x_f} \mathbb{F}(p_T). \quad (96)$$

Here,

$$\begin{aligned} \mathbb{F}(p_T) &= \sqrt{\frac{\lambda}{2\pi D}} \int_{-\infty}^{+\infty} dx_0 e^{ip_T e^{-\lambda T} x_0 - \frac{D p_T^2}{2\lambda} (1 - e^{-2\lambda T})} \mathbb{G}(p_T) e^{-\frac{\lambda}{2D} x_0^2} \\ &= e^{-\frac{D}{2\lambda} p_T^2} \left[\frac{1 + a_0^2 p_T^2 e^{-2\lambda T}}{1 + a_0^2 p_T^2} \right]^{\frac{1}{2\tilde{\tau}}}. \end{aligned} \quad (97)$$

Using Eq. (94) in Eq. (22) we have computed second and fourth moment and obtain non-Gaussian parameter by virtue of relation (24). The MSD is given as

$$\langle x^2(T) \rangle = \frac{D}{\lambda} + \frac{D_A}{\lambda}(1 - e^{-2\lambda T}), \quad (98)$$

and the fourth moment can be expressed as

$$\langle x^4(T) \rangle = 3 \langle x^2(T) \rangle^2 + 6 D_A \frac{a^2}{\lambda} (1 - e^{-4T\lambda}).$$

For the time limit $T < \tau_r$, dynamics is diffusive as

$$\langle x^2(T) \rangle = 2 D_A T + D \tau_r.$$

For very large T limit,

$$\langle x^2(T) \rangle = (D + D_A) \tau_r.$$

MSD is independent of time at very large time suggesting that the system reaches to a steady state. The NGP, γ_{np} is determined using Eq. (24) and it is given as

$$\begin{aligned} \gamma_{np} &= \frac{6 D_A \frac{a^2}{\lambda} (1 - e^{-4T\lambda})}{3 \left(\frac{D}{\lambda} + \frac{D_A}{\lambda} (1 - e^{-2\lambda T}) \right)^2} \\ &= \frac{4 \tilde{\tau} D_A^2 \sinh(2\lambda T)}{\left((D + 2D_A) \sinh(\lambda T) + D \cosh(\lambda T) \right)^2} \\ &= \frac{4 \tilde{\tau} \epsilon_A^2 \sinh(2\tilde{T})}{\left((1 + 2\epsilon_A) \sinh(\tilde{T}) + \cosh(\tilde{T}) \right)^2}. \end{aligned} \quad (99)$$

Here we have described the ratio of two diffusivities by a dimensionless parameter ϵ_A which is given as: $\epsilon_A = \frac{D_A}{D}$ and defining a dimensionless parameter \tilde{T} as $\tilde{T} = \lambda T$. At small time limit γ_{np} vanishes suggesting Gaussian behavior of PDF.

From Fig. 12 one can observe that γ_{np} starts from zero and initially increases with time. At an intermediate time it attains a peak indicating strong non-Gaussian characteristics. Then it keep decreasing and converges to a finite positive non-zero constant value of $\frac{2\tilde{\tau}\epsilon_A^2}{(1+\epsilon_A)^2}$. It implies that the distribution attains a steady state which is non-Gaussian having slow-decaying tail compared to Gaussian.

The full description of the dynamics can be investigated by computing probability distribution function (PDF). At this stage we have made the propagator dimensionless by defining some dimensionless variables as: $\tilde{T} = \frac{T}{\tau_r}$, $\tilde{x}_f = \frac{x_f}{a_0}$, $\tilde{p}_T = p_T a_0$. So the propagator becomes

$$\mathbb{P}(\tilde{x}_f, \tilde{T}) = \frac{1}{2\pi} \int_{-\infty}^{+\infty} d\tilde{p}_T e^{-i\tilde{p}_T \tilde{x}_f} \mathbb{F}(\tilde{p}_T), \quad (100)$$

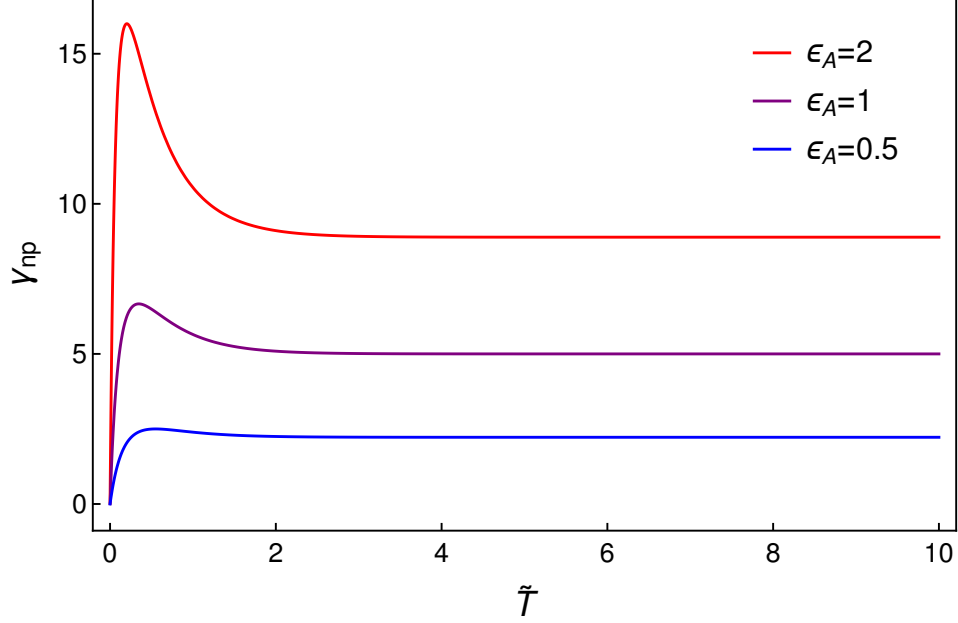


Figure 12. Non-Gaussian parameter (γ_{np}) is plotted as a function of scaled time \tilde{T} for three different values of ϵ_A at $\tilde{\tau} = 10$. The feature of distribution curve remains unchanged for any values of $\tilde{\tau}$.

where

$$\mathbb{F}(\tilde{p}_T) = e^{-\frac{\tilde{p}_T^2}{2\epsilon_A \tilde{\tau}}} \left[\frac{1 + \tilde{p}_T^2 e^{-2\tilde{T}}}{1 + \tilde{p}_T^2} \right]^{\frac{1}{2\tilde{\tau}}}. \quad (101)$$

From Eq. (100) it is clear that the PDF cannot be calculated analytically. However one can consider different time scales as discussed below.

1. *Short time* ($\tilde{T} \ll 1$).

At small time and position region *i.e.* at the limit $\tilde{p}_T^2 \gg 1$ and $\tilde{T} \ll 1$, one can approximate the characteristic functional $\mathbb{F}(\tilde{p}_T)$ in Eq. (101) as

$$\mathbb{F}(\tilde{p}_T) \sim e^{-\frac{\tilde{p}_T^2}{2\epsilon_A \tilde{\tau}} - \frac{\tilde{T}}{\tilde{\tau}}}, \quad (102)$$

which gives

$$\mathbb{P}(\tilde{x}_f, \tilde{T}) \sim \sqrt{\frac{\epsilon_A \tilde{\tau}}{2\pi}} e^{-\frac{\epsilon_A \tilde{\tau}}{2} \tilde{x}_f^2 - \frac{\tilde{T}}{\tilde{\tau}}}. \quad (103)$$

Therefore the distribution is Gaussian at small \tilde{x}_f whose strength is decaying in time due to the effect of active noise.

2. *Intermediate time.*

At small displacement region, *i.e.*, at $\tilde{x}_f \ll 1$, $\tilde{p}_T \gg 1$ and $\mathbb{F}(\tilde{p}_T) \sim e^{-\frac{\tilde{p}_T^2}{2\epsilon_A \tilde{\tau}} - \frac{\tilde{T}}{\tilde{\tau}}}$. Therefore the distribution near the origin is

$$\mathbb{P}(\tilde{x}_f, \tilde{T}) \sim \sqrt{\frac{\epsilon_A \tilde{\tau}}{2\pi}} e^{-\frac{\epsilon_A \tilde{\tau}}{2} \tilde{x}_f^2 - \frac{\tilde{T}}{\tilde{\tau}}}. \quad (104)$$

In order to get the distribution for other values of \tilde{x}_f , one write

$$\left[\frac{1 + \tilde{p}_T^2 e^{-2\tilde{T}}}{1 + \tilde{p}_T^2} \right]^{\frac{1}{2\tilde{\tau}}} = \left[e^{-2\tilde{T}} + \frac{1 - e^{-2\tilde{T}}}{1 + \tilde{p}_T^2} \right]^{\frac{1}{2\tilde{\tau}}}, \quad (105)$$

and expand as the following binomial series:

$$\left[e^{-2\tilde{T}} + \frac{1 - e^{-2\tilde{T}}}{1 + \tilde{p}_T^2} \right]^{\frac{1}{2\tilde{\tau}}} = \sum_{n=0}^{n=\infty} \binom{\frac{1}{2\tilde{\tau}}}{n} \left(e^{-2\tilde{T}} \right)^{\frac{1}{2\tilde{\tau}} - n} \frac{(1 - e^{-2\tilde{T}})^n}{(1 + \tilde{p}_T^2)^n}. \quad (106)$$

Using the convolution theorem (Eq. (26)) with the help of Eq. (43)-(44), one can rewrite the propagator in Eq. (100) as

$$\begin{aligned} \mathbb{P}(\tilde{x}_f, \tilde{T}) &= \sqrt{\frac{\epsilon_A \tilde{\tau}}{2\pi}} e^{-\frac{\tilde{T}}{\tilde{\tau}} - \frac{\epsilon_A \tilde{\tau}}{2} \tilde{x}_f^2} \\ &+ \frac{1}{2\pi} \sum_{n=1}^{\infty} \binom{\frac{1}{2\tilde{\tau}}}{n} e^{-\frac{\tilde{T}}{\tilde{\tau}}} \left(e^{2\tilde{T}} - 1 \right)^n \int_{-\infty}^{\infty} d\tilde{x} \frac{2^{\frac{3}{2}-n} \sqrt{\pi} |\tilde{x}|^{n-\frac{1}{2}} K_{n-\frac{1}{2}}(|\tilde{x}|)}{\Gamma(n)} \sqrt{\frac{\epsilon_A \tilde{\tau}}{2\pi}} e^{-\epsilon_A \tilde{\tau} (\tilde{x}_f - \tilde{x})^2 / 2}. \end{aligned} \quad (107)$$

Now considering if the Gaussian has a much narrower width than the Bessel function, *i.e.*, $\epsilon_A \tilde{\tau} \gg 1$, one can approximate the Gaussian as a delta function, and then from Eq. (107) one has

$$\begin{aligned} \mathbb{P}(\tilde{x}_f, \tilde{T}) &= \sqrt{\frac{\epsilon_A \tilde{\tau}}{2\pi}} e^{-\frac{\tilde{T}}{\tilde{\tau}} - \frac{\epsilon_A \tilde{\tau}}{2} \tilde{x}_f^2} \\ &+ \frac{1}{2\pi} \sum_{n=1}^{\infty} \binom{\frac{1}{2\tilde{\tau}}}{n} e^{-\frac{\tilde{T}}{\tilde{\tau}}} \left(e^{2\tilde{T}} - 1 \right)^n \frac{2^{\frac{3}{2}-n} \sqrt{\pi} |\tilde{x}_f|^{n-\frac{1}{2}} K_{n-\frac{1}{2}}(|\tilde{x}_f|)}{\Gamma(n)}. \end{aligned} \quad (108)$$

Strictly speaking the expansion of Eq. (106) requires $e^{-2\tilde{T}} > (1 - e^{-2\tilde{T}})$ or $\tilde{T} < \ln(2)/2$. However, the expansion of Eq. (108) seems to be valid for other values of \tilde{T} too.

To get the tail behavior of the distribution, one can use the asymptotic form for the Bessel function $K_n(|\tilde{x}_f|) \approx \sqrt{\frac{\pi}{2|\tilde{x}_f|}} e^{-|\tilde{x}_f|}$ in the above, and thereafter summing over n one

can obtain

$$\mathbb{P}(\tilde{x}_f, \tilde{T}; \tilde{x}_0 = 0, 0) = \sqrt{\frac{\epsilon_A \tilde{\tau}}{2\pi}} e^{-\frac{\epsilon_A \tilde{\tau}}{2} \tilde{x}_f^2 - \frac{\tilde{T}}{\tilde{\tau}}} + \frac{e^{-|\tilde{x}_f| - \frac{\tilde{T}}{\tilde{\tau}}}}{4\tilde{\tau}} \left(e^{2\tilde{T}} - 1 \right) {}_1F_1 \left(1 - \frac{1}{2\tilde{\tau}}; 2; -\frac{1}{2}(e^{2\tilde{T}} - 1) |\tilde{x}_f| \right). \quad (109)$$

So the distribution has a Gaussian core near the origin as given by the first term on the right-hand side of Eq. (109). The second term signifies the departure from Gaussianity, which decays like

$$\mathbb{P}(\tilde{x}_f, \tilde{T}) \sim \frac{2^{1-\frac{1}{2\tilde{\tau}}} (e^{2\tilde{T}} - 1)^{\frac{1}{2\tilde{\tau}}}}{\Gamma(1 + \frac{1}{2\tilde{\tau}}) |\tilde{x}_f|^{1-\frac{1}{2\tilde{\tau}}}} \frac{e^{-|\tilde{x}_f| - \frac{\tilde{T}}{\tilde{\tau}}}}{4\tilde{\tau}}.$$

This analytical result is in agreement with numerical calculations, as shown in Fig. 13.

To capture the sensitivity of initial distribution on dynamics at transient period, one can consider the particle's initial distribution as a delta function (i.e. $\delta(x_0)$) and hence, Eq. (96) can be reconstructed as

$$\mathbb{P}(x_f, T) = \frac{1}{2\pi} \int_{-\infty}^{+\infty} dp_T e^{-ip_T x_f} \mathbb{F}(p_T), \quad (110)$$

with

$$\mathbb{F}(p_T) = e^{-\frac{D p_T^2}{2\lambda}(1-e^{-2\lambda T})} \left[\frac{1 + a_0^2 p_T^2 e^{-2\lambda T}}{1 + a_0^2 p_T^2} \right]^{\frac{1}{2\tilde{\tau}}}. \quad (111)$$

Upon rescaling as earlier, the above can be expressed as

$$\mathbb{P}(\tilde{x}_f, \tilde{T}) = \frac{1}{2\pi} \int_{-\infty}^{+\infty} d\tilde{p}_T e^{-i\tilde{p}_T \tilde{x}_f} e^{-\frac{\tilde{p}_T^2}{2\epsilon_A \tilde{\tau}}(1-e^{-2\tilde{T}})} \left[\frac{1 + \tilde{p}_T^2 e^{-2\tilde{T}}}{1 + \tilde{p}_T^2} \right]^{\frac{1}{2\tilde{\tau}}}, \quad (112)$$

which can be rewritten as

$$\begin{aligned} \mathbb{P}(\tilde{x}_f, \tilde{T}) &= \sqrt{\frac{\epsilon_A \tilde{\tau}}{2(1-e^{-2\tilde{T}})}} \frac{1}{\pi} e^{-\frac{\tilde{T}}{\tilde{\tau}} - \frac{\epsilon_A \tilde{\tau}}{2(1-e^{-2\tilde{T}})} \tilde{x}_f^2} \\ &+ \frac{1}{2\pi} \sum_{n=1}^{\infty} \left(\frac{1}{2\tilde{\tau}} \right)^n e^{-\frac{\tilde{T}}{\tilde{\tau}}} (e^{2\tilde{T}} - 1)^n \int_{-\infty}^{\infty} d\tilde{x} \frac{2^{\frac{3}{2}-n} \sqrt{\pi} |\tilde{x}|^{n-\frac{1}{2}} K_{n-\frac{1}{2}}(|\tilde{x}|)}{\Gamma(n)} \sqrt{\frac{\epsilon_A \tilde{\tau}}{2\pi}} e^{-\frac{\epsilon_A \tilde{\tau}}{2(1-e^{-2\tilde{T}})} (\tilde{x}_f - \tilde{x})^2}. \end{aligned} \quad (113)$$

Therefore similar to the previous analysis, in the limit $\frac{\epsilon_A \tilde{\tau}}{\tilde{T}} \gg 1$, the distribution can be given as

$$\begin{aligned} \mathbb{P}(\tilde{x}_f, \tilde{T}; \tilde{x}_0 = 0, 0) &\approx \sqrt{\frac{\epsilon_A \tilde{\tau}}{2(1-e^{-2\tilde{T}})}} \frac{1}{\pi} e^{-\frac{\tilde{T}}{\tilde{\tau}} - \frac{\epsilon_A \tilde{\tau}}{2(1-e^{-2\tilde{T}})} \tilde{x}_f^2} \\ &+ \frac{e^{-|\tilde{x}_f| - \frac{\tilde{T}}{\tilde{\tau}}}}{4\tilde{\tau}} (e^{2\tilde{T}} - 1) {}_1F_1 \left(1 - \frac{1}{2\tilde{\tau}}; 2; -\frac{1}{2}(e^{2\tilde{T}} - 1) |\tilde{x}_f| \right). \end{aligned} \quad (114)$$

So, the choice of different initial conditions only modifies the central core but the tail behavior remains unchanged.

3. Long time, $\tilde{T} \gg 1$.

At long time limit, Eq. (101) can be simplified by taking $e^{-2\tilde{T}} \rightarrow 0$, and approximating $\mathbb{F}(p_T)$ as

$$\mathbb{F}(\tilde{p}_T) \approx e^{-\frac{\tilde{p}_T^2}{2\epsilon_A \tilde{\tau}}} \left(\frac{1}{1 + \tilde{p}_T^2} \right)^{\frac{1}{2\tilde{\tau}}}. \quad (115)$$

Hence, the distribution becomes

$$\mathbb{P}(\tilde{x}_f, \tilde{T}) = \frac{1}{2\pi} \int_{-\infty}^{+\infty} d\tilde{p}_T e^{-i\tilde{p}_T \tilde{x}_f} e^{-\frac{\tilde{p}_T^2}{2\epsilon_A \tilde{\tau}}} \left(\frac{1}{1 + \tilde{p}_T^2} \right)^{\frac{1}{2\tilde{\tau}}}. \quad (116)$$

3.1. $\tilde{x}_f \ll 1$

In small \tilde{x}_f limit, $\tilde{p}_T^2 \gg 1$. So, it allows us to approximate $\mathbb{F}(\tilde{p}_T)$ as

$$\mathbb{F}(\tilde{p}_T) \approx e^{-\frac{\tilde{p}_T^2}{2\epsilon_A \tilde{\tau}}} [\tilde{p}_T^2]^{-\frac{1}{2\tilde{\tau}}}. \quad (117)$$

After performing the inverse Fourier transform of relation (117) with the assumption $\tilde{\tau} > 1$, one can obtain the PDF and it reads

$$\mathbb{P}(\tilde{x}_f) = \frac{\Gamma(\frac{1}{2} - \frac{1}{2\tilde{\tau}})}{2\pi} \left(\frac{1}{2\epsilon_A \tilde{\tau}} \right)^{-\frac{1}{2}(1-1/\tilde{\tau})} {}_1F_1 \left(\frac{1}{2} - \frac{1}{2\tilde{\tau}}; \frac{1}{2}; -\epsilon_A \frac{\tilde{\tau} \tilde{x}_f^2}{2} \right). \quad (118)$$

We have encountered the same kind of distribution in the section III D and have seen that near to the origin, distribution is Gaussian of the form:

$$\mathbb{P}(\tilde{x}_f) \sim e^{-\frac{\epsilon_A \tilde{\tau}}{2} \tilde{x}_f^2}. \quad (119)$$

3.2. Intermediate \tilde{x}_f

To get the tail behavior, Eq. (116) is required to be evaluated which unfortunately cannot be done directly. However it can be rewritten as convolution of two functions in Fourier domain as discussed in section III C as well as in section III D. So, PDF in Eq. (100) can be expressed as

$$\mathbb{P}(\tilde{x}_f) = \int_{-\infty}^{+\infty} d\tilde{x} \sqrt{\frac{\epsilon_A \tilde{\tau}}{2\pi}} e^{-\frac{\epsilon_A \tilde{\tau}}{2} (\tilde{x}_f - \tilde{x})^2} \times \frac{2^{\frac{3}{2} - \frac{1}{2\tilde{\tau}}} \sqrt{\pi} |\tilde{x}|^{\frac{1}{2\tilde{\tau}} - \frac{1}{2}} K_{\frac{1}{2\tilde{\tau}} - \frac{1}{2}}(|\tilde{x}|)}{\Gamma(\frac{1}{2\tilde{\tau}})}. \quad (120)$$

For $\epsilon_A \tilde{\tau} \gg 1$, one can replace Gaussian distribution with a delta function as

$$\sqrt{\frac{\epsilon_A \tilde{\tau}}{2\pi}} e^{-\frac{\epsilon_A \tilde{\tau}}{2} (\tilde{x}-\tilde{y})^2} \approx \delta(\tilde{x} - \tilde{y}).$$

Therefore, the approximate distribution is given by

$$\mathbb{P}(\tilde{x}_f) \approx \frac{2^{\frac{1}{2}-\frac{1}{2\tilde{\tau}}} |\tilde{x}_f|^{\frac{1}{2\tilde{\tau}}-\frac{1}{2}} K_{\frac{1}{2\tilde{\tau}}-\frac{1}{2}}(|\tilde{x}_f|)}{\sqrt{\pi} \Gamma(\frac{1}{2\tilde{\tau}})}. \quad (121)$$

So, the distribution has an exponential tail of the form : $e^{-|\tilde{x}_f|}$. In fact at $\tilde{T} \rightarrow \infty$ limit and for $2\tilde{\tau} = 1$ one can compute the distribution exactly as discussed in Appendix C and the probability is given in Eq. (C4). It is conspicuous that the probability decays exponentially at large displacement and this is true for any values of $\tilde{\tau}$. However, the distribution for $2\tilde{\tau} = 1$ does not contain any attributes of Eq. (118). As we are interested to know the steady state distribution we have considered $\tilde{T} \rightarrow \infty$ limit for different values of $\tilde{\tau}$ and have performed numerical integration of relation (C3) and get PDF vs. displacement plot as shown in Fig. 14. The plots are in accord with our analytical findings.

V. CONCLUSION

In the first part of the paper, we studied the diffusion of a free particle subject to both white and active noise. As expected, we have seen that in the case where both thermal and active noises are Gaussian, the PDF for the displacement of the particle is always Gaussian. A system driven by active dichotomous noise, too gives a Gaussian distribution at long time scales. In the case where active noise is dominant over the thermal noise, the approach to one single Gaussian distribution at long times is through the spreading of two Gaussians peaked at $+uT$ and $-uT$, analogous to what was seen in [18]. In the case of active noise being white Poissonian, we find that the distribution is Gaussian at very large time and displacement limits as a consequence of the central limit theorem. But the initial distribution is non-Gaussian, and has a central Gaussian part with an exponential tail. This kind of distribution has been observed in some experiments [7, 8]. The presence of an exponential tail is a manifestation of Poisson noise, the amplitude of which is itself exponentially distributed. The dynamics in case of non-white (correlated) Poisson noise (results of Section III D) has been found to be fascinating. In this case the distribution for large displacements is

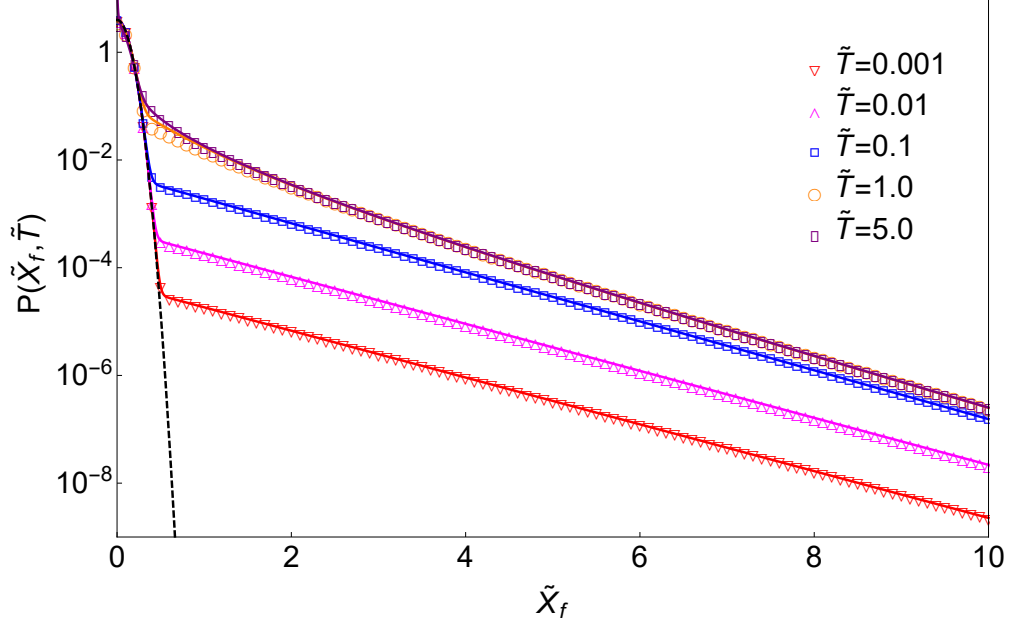


Figure 13. Logarithm of the probability distribution(PDF) function plotted against \tilde{x}_f at different timescales as presented with symbols. PDF is computed numerically for a particular set of parameters $\{\epsilon_A = 10, \tilde{\tau} = 10\}$ using Eq. (100). The solid curves are obtained using Eq. (109) which fit very well with the numerical curves. The black dotted curve is the central Gaussian part of the distribution 109.

Gaussian at long time. But in an intermediate time scale, the distribution largely deviates from Gaussianity, having a central Gaussian part with prominent exponential tail. This has also been supported by NGP calculation where NGP is found as a non-monotonic function of time and at intermediate time it attains a maximum. These results seem quite useful as such traits have been observed for diffusion process of passive particles inside cellular environment, for instance, see Ref. [5]. The method we have addressed here can be utilized, in principle, to study the dynamics in underdamped limit. In the second part we have discussed dynamics of a trapped particle. For reasons of simplicity and solvability, the potential was assumed as harmonic and the particle was initially taken to be in thermal equilibrium, with no active noise present. When the active noise is introduced into the system in the form of correlated Gaussian noise it still remains normal distributed but with an extended standard deviation which is signature of this extra noise. Here it should be mentioned that the elevation of standard deviation can be attributed to the increase of potential energy of the system as well as the local temperature, sometimes termed as 'effective temperature' [36, 54]. A confined

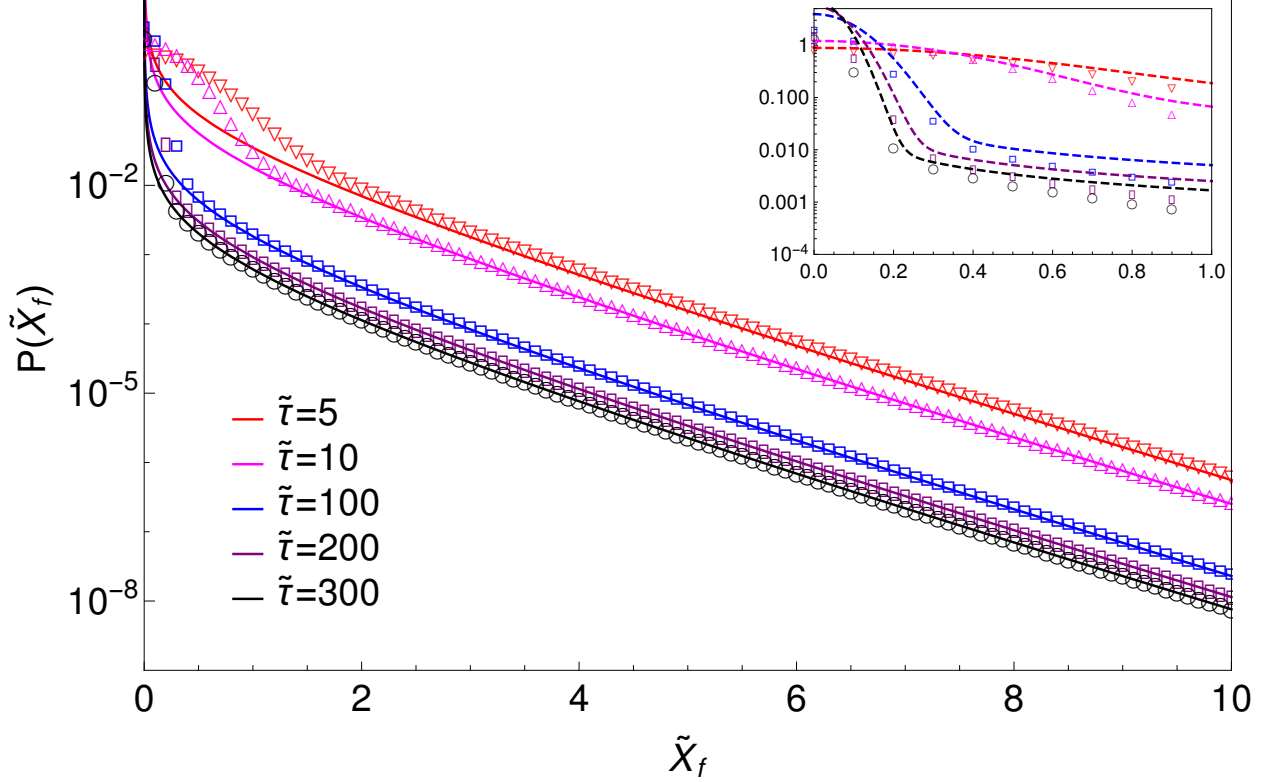


Figure 14. Logarithm of the probability distribution(PDF) function plotted against displacement for different values of $\tilde{\tau}$ at $\epsilon_A = 1$. PDF is computed numerically using Eq. (C3) and compare with Eq. (121) (solid lines) which are well fitted at intermediate to long displacement limit. At short distance, those agree well with Eq. (118)(dashed curves) as shown in inset.

system in dichotomous noise replicates the dynamics of self propelled particles for which case the probability is mainly concentrated near $\pm u/\lambda$ at steady state. In the case where the active noise is modeled as Poissonian white noise, the distribution strongly deviates from Gaussian behavior as time passes and at stationary limit it attains a distribution which decays exponentially with distance from equilibrium position. This is an obvious demonstration of out-of-equilibrium state. Clearly this system is an ideal choice to study useful thermodynamic properties (*e.g.*, heat, work, entropy) of optically trapped particle in an active bath [49, 55].

VI. ACKNOWLEDGMENTS

Koushik would like to acknowledge IISc for financial support. The work of KLS was supported by the J.C. Bose Fellowship of the Department of Science and Technology, Govt. of India.

Appendix A: Limiting forms of PDF in the case where the active noise is dichotomous

In the following, we study the short term, as well as long term limits of the probability distribution given as a convolution in Eq. (29). The first term of inverse Fourier transform (IFT) given in Eq. (31) is a delta function. So its convolution with Eq. (30) is easy and the result is

$$\begin{aligned} P_1 &= \sqrt{\frac{\epsilon_A}{4\pi\tilde{T}}} \int_{-\infty}^{+\infty} d\tilde{x}' e^{-\frac{\epsilon_A(\tilde{x}-\tilde{x}')^2}{4\tilde{T}}} \frac{e^{-\frac{\tilde{T}}{2}}}{2} [\delta(\tilde{x}' + \tilde{T}) + \delta(\tilde{x}' - \tilde{T})] \\ &= \sqrt{\frac{\epsilon_A e^{-\tilde{T}}}{16\pi\tilde{T}}} \left[e^{-\frac{\epsilon_A(\tilde{x}-\tilde{T})^2}{4\tilde{T}}} + e^{-\frac{\epsilon_A(\tilde{x}+\tilde{T})^2}{4\tilde{T}}} \right]. \end{aligned} \quad (\text{A1})$$

The second and third term of IFT in Eq. (31) contain modified Bessel functions of first kind of zero and first order, respectively. One can write the Modified Bessel function $I_n(x)$ of integer order n , as an integral representation [56]

$$I_n(x) = \frac{1}{\pi} \int_0^\pi d\theta e^{x \cos\theta} \cos n\theta. \quad (\text{A2})$$

The evaluation of the term involving I_0 is discussed below.

$$\begin{aligned} P_2 &= \sqrt{\frac{\epsilon_A}{4\pi\tilde{T}}} \int_{-\infty}^{+\infty} d\tilde{x}' e^{-\frac{\epsilon_A(\tilde{x}-\tilde{x}')^2}{4\tilde{T}}} \frac{e^{-\frac{\tilde{T}}{2}}}{4} [\theta(\tilde{x}' + \tilde{T}) - \theta(\tilde{x}' - \tilde{T})] I_0 \left[\frac{\tilde{T}}{2} \sqrt{1 - \left(\frac{\tilde{x}'}{\tilde{T}}\right)^2} \right] \\ &= \sqrt{\frac{\epsilon_A e^{-\tilde{T}}}{64\pi\tilde{T}}} \int_{-\tilde{T}}^{+\tilde{T}} d\tilde{x}' e^{-\frac{\epsilon_A(\tilde{x}-\tilde{x}')^2}{4\tilde{T}}} I_0 \left[\frac{\tilde{T}}{2} \sqrt{1 - \left(\frac{\tilde{x}'}{\tilde{T}}\right)^2} \right] \end{aligned}$$

After taking $\frac{\tilde{x}'}{\tilde{T}} = \sin\phi$ and rewriting P_1 using relation (A2) one can arrive at

$$\begin{aligned} P_2 &= \frac{1}{\pi} \sqrt{\frac{\epsilon_A \tilde{T} e^{-\tilde{T}}}{64\pi}} \int_{-\frac{\pi}{2}}^{+\frac{\pi}{2}} d\phi \cos\phi \int_0^\pi d\theta e^{-\frac{\epsilon_A(\tilde{x}-\tilde{T}\sin\phi)^2}{4\tilde{T}}} e^{\frac{\tilde{T}}{2} \cos\phi \cos\theta} \\ &= \frac{1}{\pi} \sqrt{\frac{\epsilon_A \tilde{T} e^{-\tilde{T}}}{64\pi}} \int_{-\frac{\pi}{2}}^{+\frac{\pi}{2}} d\phi \cos\phi \int_0^\pi d\theta e^{\frac{\tilde{T}}{2} \cos\phi \cos\theta - \frac{\epsilon_A \tilde{x}^2}{4\tilde{T}} - \frac{\epsilon_A \tilde{T} \sin^2\phi}{4} + \frac{\epsilon_A \tilde{x}}{2} \sin\phi}. \end{aligned} \quad (\text{A3})$$

Similarly for term involving $I_1(x)$,

$$\begin{aligned}
P_3 &= \sqrt{\frac{\epsilon_A}{4\pi\tilde{T}}} \int_{-\infty}^{+\infty} d\tilde{x}' e^{-\frac{\epsilon_A(\tilde{x}-\tilde{x}')^2}{4\tilde{T}}} \frac{e^{-\frac{\tilde{T}}{2}}}{4} \frac{[\theta(\tilde{x}' + \tilde{T}) - \theta(\tilde{x}' - \tilde{T})]}{\sqrt{1 - \left(\frac{\tilde{x}'}{\tilde{T}}\right)^2}} I_1 \left[\frac{\tilde{T}}{2} \sqrt{1 - \left(\frac{\tilde{x}'}{\tilde{T}}\right)^2} \right] \\
&= \sqrt{\frac{\epsilon_A e^{-\tilde{T}}}{64\pi\tilde{T}}} \int_{-\tilde{T}}^{+\tilde{T}} d\tilde{x}' \frac{e^{-\frac{\epsilon_A(\tilde{x}-\tilde{x}')^2}{4\tilde{T}}}}{\sqrt{1 - \left(\frac{\tilde{x}'}{\tilde{T}}\right)^2}} I_1 \left[\frac{\tilde{T}}{2} \sqrt{1 - \left(\frac{\tilde{x}'}{\tilde{T}}\right)^2} \right] \\
&= \frac{1}{\pi} \sqrt{\frac{\epsilon_A \tilde{T} e^{-\tilde{T}}}{64\pi}} \int_{-\frac{\pi}{2}}^{+\frac{\pi}{2}} d\phi \int_0^\pi d\theta \cos\theta e^{\frac{\tilde{T}}{2} \cos\phi \cos\theta - \frac{\epsilon_A \tilde{x}^2}{4\tilde{T}} - \frac{\epsilon_A \tilde{T} \sin^2\phi}{4} + \frac{\epsilon_A \tilde{x}}{2} \sin\phi}. \tag{A4}
\end{aligned}$$

a. Small time limit

Let us consider the limit $\tilde{T} \ll 1$. At this temporal regime in Eq. (A3) we can expand the term $e^{\frac{\tilde{T}}{2} \cos\phi \cos\theta}$ and keeping only first two terms one can approximate P_2 as follows:

$$\begin{aligned}
P_2 &= \frac{1}{\pi} \sqrt{\frac{\epsilon_A \tilde{T} e^{-\tilde{T}}}{64\pi}} \int_{-\frac{\pi}{2}}^{+\frac{\pi}{2}} d\phi \cos\phi \int_0^\pi d\theta \left(1 + \frac{\tilde{T}}{2} \cos\phi \cos\theta \right) e^{-\frac{\epsilon_A \tilde{x}^2}{4\tilde{T}} - \frac{\epsilon_A \tilde{T} \sin^2\phi}{4} + \frac{\epsilon_A \tilde{x}}{2} \sin\phi} \\
&= \sqrt{\frac{\epsilon_A \tilde{T} e^{-\tilde{T}}}{64\pi}} \int_{-\frac{\pi}{2}}^{+\frac{\pi}{2}} d\phi \cos\phi e^{-\frac{\epsilon_A \tilde{x}^2}{4\tilde{T}} - \frac{\epsilon_A \tilde{T} \sin^2\phi}{4} + \frac{\epsilon_A \tilde{x}}{2} \sin\phi} \\
&= \sqrt{\frac{\epsilon_A \tilde{T} e^{-\tilde{T}}}{64\pi}} e^{-\frac{\epsilon_A \tilde{x}^2}{4\tilde{T}}} \int_{-1}^{+1} dz e^{-\frac{\epsilon_A \tilde{T} z^2}{4} + \frac{\epsilon_A \tilde{x}}{2} z} \\
&= \sqrt{\frac{e^{-\tilde{T}}}{64}} \left[\operatorname{erf} \left(\sqrt{\frac{\epsilon_A}{4\tilde{T}}} (\tilde{x} + \tilde{T}) \right) - \operatorname{erf} \left(\sqrt{\frac{\epsilon_A}{4\tilde{T}}} (\tilde{x} - \tilde{T}) \right) \right] \tag{A5}
\end{aligned}$$

Likewise,

$$\begin{aligned}
P_3 &= \frac{1}{\pi} \sqrt{\frac{\epsilon_A \tilde{T} e^{-\tilde{T}}}{64\pi}} \int_{-\frac{\pi}{2}}^{+\frac{\pi}{2}} d\phi \int_0^\pi d\theta \cos\theta \left(1 + \frac{\tilde{T}}{2} \cos\phi \cos\theta \right) e^{-\frac{\epsilon_A \tilde{x}^2}{4\tilde{T}} - \frac{\epsilon_A \tilde{T} \sin^2\phi}{4} + \frac{\epsilon_A \tilde{x}}{2} \sin\phi} \\
&= \frac{\tilde{T}}{4} \sqrt{\frac{\epsilon_A \tilde{T} e^{-\tilde{T}}}{64\pi}} \int_{-\frac{\pi}{2}}^{+\frac{\pi}{2}} d\phi \cos\phi e^{-\frac{\epsilon_A \tilde{x}^2}{4\tilde{T}} - \frac{\epsilon_A \tilde{T} \sin^2\phi}{4} + \frac{\epsilon_A \tilde{x}}{2} \sin\phi} \\
&= \frac{\tilde{T}}{4} \sqrt{\frac{e^{-\tilde{T}}}{64}} \left[\operatorname{erf} \left(\sqrt{\frac{\epsilon_A}{4\tilde{T}}} (\tilde{x} + \tilde{T}) \right) - \operatorname{erf} \left(\sqrt{\frac{\epsilon_A}{4\tilde{T}}} (\tilde{x} - \tilde{T}) \right) \right] = \mathcal{O}(\tilde{T}^2). \tag{A6}
\end{aligned}$$

Therefore, by virtue of Eq. (A1),(A5),(A6) the probability distribution function at very short time limit is obtained as

$$\begin{aligned}
\mathbb{P}(\tilde{x}_f, \tilde{T}; \tilde{x}_0 = 0, 0) &= \sqrt{\frac{\epsilon_A e^{-\tilde{T}}}{16\pi\tilde{T}}} \left[e^{-\frac{\epsilon_A(\tilde{x}_f - \tilde{T})^2}{4\tilde{T}}} + e^{-\frac{\epsilon_A(\tilde{x}_f + \tilde{T})^2}{4\tilde{T}}} \right] \\
&+ \sqrt{\frac{e^{-\tilde{T}}}{64}} \left[\operatorname{erf} \left(\sqrt{\frac{\epsilon_A}{4\tilde{T}}}(\tilde{x}_f + \tilde{T}) \right) - \operatorname{erf} \left(\sqrt{\frac{\epsilon_A}{4\tilde{T}}}(\tilde{x}_f - \tilde{T}) \right) \right] \quad (\text{A7})
\end{aligned}$$

b. *Long time limit*

For large s , Modified Bessel function can be expanded asymptotically as

$$I_n(s) \sim \sqrt{\frac{1}{2\pi s}} e^s \quad \text{for } s \rightarrow \infty. \quad (\text{A8})$$

Using Eq. (A8) we can write down $I_n(x)$ at long \tilde{T} limit as

$$\begin{aligned}
I_n \left[\frac{\tilde{T}}{2} \sqrt{1 - \left(\frac{\tilde{x}'}{\tilde{T}} \right)^2} \right] &\sim \sqrt{\frac{1}{2\pi}} \frac{e^{\frac{\tilde{T}}{2} \sqrt{1 - \left(\frac{\tilde{x}'}{\tilde{T}} \right)^2}}}{\sqrt{\frac{\tilde{T}}{2} \sqrt{1 - \left(\frac{\tilde{x}'}{\tilde{T}} \right)^2}}} \\
&\sim \sqrt{\frac{1}{\pi\tilde{T}}} e^{\frac{\tilde{T}}{2} \left(1 - \frac{1}{2} \left(\frac{\tilde{x}'}{\tilde{T}} \right)^2 \right)} \\
&= \sqrt{\frac{e^{\tilde{T}}}{\pi\tilde{T}}} e^{-\frac{\tilde{x}'^2}{4\tilde{T}}}.
\end{aligned}$$

So, at the limit $\tilde{T} \gg 1$, P_2 becomes

$$\begin{aligned}
P_2 &= \mathcal{L}t \sqrt{\frac{\epsilon_A e^{-\tilde{T}}}{64\pi\tilde{T}}} \sqrt{\frac{e^{\tilde{T}}}{\pi\tilde{T}}} \int_{-\tilde{T}}^{+\tilde{T}} d\tilde{x}' e^{-\frac{\epsilon_A(\tilde{x} - \tilde{x}')^2}{4\tilde{T}}} e^{-\frac{\tilde{x}'^2}{4\tilde{T}}} \\
&= \sqrt{\frac{\epsilon_A}{64\pi^2\tilde{T}^2}} \int_{-\infty}^{+\infty} d\tilde{x}' e^{-\frac{\epsilon_A(\tilde{x} - \tilde{x}')^2}{4\tilde{T}}} e^{-\frac{\tilde{x}'^2}{4\tilde{T}}} \\
&= \sqrt{\frac{\epsilon_A}{64\pi^2\tilde{T}^2}} \sqrt{\frac{4\pi\tilde{T}}{1 + \epsilon_A}} e^{-\frac{\epsilon_A}{1 + \epsilon_A} \frac{\tilde{x}^2}{4\tilde{T}}} \\
&= \frac{1}{2} \sqrt{\frac{\epsilon_A}{4(1 + \epsilon_A)\pi\tilde{T}}} e^{-\frac{\epsilon_A}{1 + \epsilon_A} \frac{\tilde{x}^2}{4\tilde{T}}}. \quad (\text{A9})
\end{aligned}$$

In similar fashion,

$$P_3 = \frac{1}{2} \sqrt{\frac{\epsilon_A}{4(1 + \epsilon_A)\pi\tilde{T}}} e^{-\frac{\epsilon_A}{1 + \epsilon_A} \frac{\tilde{x}^2}{4\tilde{T}}}. \quad (\text{A10})$$

For $\tilde{T} \rightarrow \infty$,

$$P_1 = \mathcal{L}t \sqrt{\frac{\epsilon_A e^{-\tilde{T}}}{16\pi\tilde{T}}} \left[e^{-\frac{\epsilon_A(\tilde{x} - \tilde{T})^2}{4\tilde{T}}} + e^{-\frac{\epsilon_A(\tilde{x} + \tilde{T})^2}{4\tilde{T}}} \right] \rightarrow 0.$$

Therefore, from Eq. (29) one can obtain the probability distribution function at large time limit as

$$\mathbb{P}(\tilde{x}_f, \tilde{T}; \tilde{x}_0 = 0, 0) = \sqrt{\frac{\epsilon_A}{4(1 + \epsilon_A) \pi \tilde{T}}} e^{-\frac{\epsilon_A}{1 + \epsilon_A} \frac{\tilde{x}^2}{4\tilde{T}}}. \quad (\text{A11})$$

Appendix B: Moments of $\sigma_{PC}(t)$ and its expression in terms of $\sigma_{PW}(t)$

Using Eq. (50) one can express $\sigma_{PC}(t)$ in terms of $\sigma_{PW}(t)$ as

$$\begin{aligned} \sigma_{PC}(t) &= \lambda_p \int_{-\infty}^t ds e^{-\lambda_p(t-s)} \sigma_{PW}(s) \\ &= \lambda_p \int_{-\infty}^{+\infty} ds \Theta(t-s) e^{-\lambda_p(t-s)} \sigma_{PW}(s). \end{aligned}$$

So the second order correlation can be written as

$$\begin{aligned} \langle \sigma_{PC}(t_1) \sigma_{PC}(t_2) \rangle &= \lambda_p^2 \int_{-\infty}^{+\infty} ds_1 \int_{-\infty}^{+\infty} ds_2 \Theta(t_1 - s_1) \Theta(t_2 - s_2) e^{-\lambda_p(t_1 - s_1 + t_2 - s_2)} \\ &\quad \langle \sigma_{PW}(s_1) \sigma_{PW}(s_2) \rangle. \end{aligned} \quad (\text{B1})$$

Using the auto-correlation of $\sigma_{PW}(t)$ as given in Eq. (34) and integrating over s_1 we reach at

$$\langle \sigma_{PC}(t_1) \sigma_{PC}(t_2) \rangle = 2D_A \lambda_p^2 \int_{-\infty}^{+\infty} ds_2 \Theta(t_1 - s_2) \Theta(t_2 - s_2) e^{-\lambda_p(t_1 + t_2 - 2s_2)}, \quad (\text{B2})$$

which follows

$$\begin{aligned} \langle \sigma_{PC}(t_1) \sigma_{PC}(t_2) \rangle &= 2D_A \lambda_p^2 \int_{-\infty}^{\min(t_1, t_2)} ds_2 \Theta(t_1 - s_2) \Theta(t_2 - s_2) e^{-\lambda_p(t_1 + t_2 - 2s_2)} \\ &= D_A \lambda_p e^{-\lambda_p |t_1 - t_2|} \\ &= \frac{D_A}{\tau_p} e^{-|t_1 - t_2| / \tau_p}. \end{aligned} \quad (\text{B3})$$

τ_p is correlation (or persistence) time of active noise which is defined as $\tau_p = \frac{1}{\lambda_p}$. Note that, at the limit $\tau_p \rightarrow 0$, σ_{PC} tends to σ_{PW} as it is anticipated from Eq. (50) and the correlation becomes delta-correlated as one can obtain from Eq. (B3), taking the said limit.

In Eq. (51) we have expressed characteristic function of $\sigma_{PC}(t)$ in terms of $\sigma_{PW}(t)$ which

we have obtained as follows:

$$\begin{aligned}
\int_0^T dt \sigma_{PC}(t) &= \lambda_p \int_0^T dt \int_{-\infty}^{+\infty} ds \Theta(t-s) e^{-\lambda_p(t-s)} \sigma_{PW}(s) \\
&= \lambda_p \int_{-\infty}^{+\infty} ds \int_{-\infty}^{+\infty} dt \Theta(t-s) \Theta(T-s) \Theta(t) \Theta(T-t) e^{\lambda_p s} e^{-\lambda_p t} \sigma_{PW}(s) \\
&= \int_{-\infty}^{+\infty} ds \Theta(T-s) e^{\lambda_p s} \sigma_{PW}(s) (e^{-\lambda_p \max(0,s)} - e^{-\lambda_p T}) \\
&= \int_{-\infty}^{+\infty} ds e^{\lambda_p s} (1 - e^{-\lambda_p T}) \sigma_{PW}(s); \text{ if } s < 0 \\
&= \int_{-\infty}^{+\infty} ds (1 - e^{-\lambda_p(T-s)}) \sigma_{PW}(s); \text{ if } T \geq s \geq 0.
\end{aligned} \tag{B4}$$

Appendix C: Calculation of stationary probability distribution function for $\tilde{\tau} = 0.5$

Stationary distribution can be obtained by considering the limit $\tilde{T} \rightarrow \infty$. In this limit, Eq. (100) becomes

$$\mathbb{P}(\tilde{x}_f) = \frac{1}{2\pi} \int_{-\infty}^{+\infty} d\tilde{p}_T e^{-i\tilde{p}_T \tilde{x}_f} e^{-\frac{\tilde{p}_T^2}{2\epsilon_A \tilde{\tau}}} \left[\frac{1}{1 + \tilde{p}_T^2} \right]^{\frac{1}{2\tilde{\tau}}}. \tag{C1}$$

Using the identity

$$\left[\frac{1}{1 + \tilde{p}_T^2} \right]^{\frac{1}{2\tilde{\tau}}} = \frac{1}{\Gamma(\frac{1}{2\tilde{\tau}})} \int_0^\infty e^{-(1+\tilde{p}_T^2)s} s^{\frac{1}{2\tilde{\tau}}-1} ds, \tag{C2}$$

in the above equation and doing the Fourier inversion with respect to \tilde{p}_T (which is essentially a Gaussian integration) we arrive at

$$\mathbb{P}(\tilde{x}_f) = \frac{1}{\Gamma(\frac{1}{2\tilde{\tau}})} \int_0^\infty \frac{s^{\frac{1}{2\tilde{\tau}}-1} e^{-s - \frac{\tilde{x}_f^2}{4(\alpha+s)}}}{\sqrt{4\pi(\alpha+s)}} ds, \tag{C3}$$

where $\alpha = \frac{1}{2\epsilon_A \tilde{\tau}}$. For $2\tilde{\tau} = 1$, the above integration can be performed exactly which leads to the following result:

$$\mathbb{P}(\tilde{x}_f) = \frac{1}{4} e^{-|\tilde{x}_f| + \alpha} \left[2 - \operatorname{erfc} \left(\frac{|\tilde{x}_f| - 2\alpha}{2\sqrt{\alpha}} \right) + e^{2|\tilde{x}_f|} \operatorname{erfc} \left(\frac{|\tilde{x}_f| + 2\alpha}{2\sqrt{\alpha}} \right) \right]. \tag{C4}$$

[1] N. G. Van Kampen, Stochastic processes in physics and chemistry, vol. 1 (Elsevier, 1992).

- [2] A. Einstein, Investigations on the Theory of the Brownian Movement (Courier Corporation, 1956).
- [3] E. Frey and K. Kroy, *Annalen der Physik* **14**, 20 (2005).
- [4] D. Mizuno, C. Tardin, C. F. Schmidt, and F. C. MacKintosh, *Science* **315**, 370 (2007).
- [5] T. Toyota, D. A. Head, C. F. Schmidt, and D. Mizuno, *Soft Matter* **7**, 3234 (2011).
- [6] B. Stuhrmann, M. S. e Silva, M. Depken, F. C. MacKintosh, and G. H. Koenderink, *Phys. Rev. E* **86**, 020901 (2012).
- [7] É. Fodor, M. Guo, N. Gov, P. Visco, D. Weitz, and F. van Wijland, *EPL* **110**, 48005 (2015).
- [8] K. C. Leptos, J. S. Guasto, J. P. Gollub, A. I. Pesci, and R. E. Goldstein, *Phys. Rev. Lett.* **103**, 198103 (2009), URL <https://link.aps.org/doi/10.1103/PhysRevLett.103.198103>.
- [9] P. Mestres, I. A. Martinez, A. Ortiz-Ambriz, R. A. Rica, and E. Roldan, *Phys. Rev. E* **90**, 032116 (2014).
- [10] V. Berdichevsky and M. Gitterman, *Phys. Rev. E* **60**, 1494 (1999), URL <https://link.aps.org/doi/10.1103/PhysRevE.60.1494>.
- [11] R. Rozenfeld, A. Neiman, and L. Schimansky-Geier, *Phys. Rev. E* **62**, R3031 (2000), URL <https://link.aps.org/doi/10.1103/PhysRevE.62.R3031>.
- [12] J.-h. Li and Y.-x. Han, *Phys. Rev. E* **74**, 051115 (2006), URL <https://link.aps.org/doi/10.1103/PhysRevE.74.051115>.
- [13] M. R. Roussel and J. Wang, *J. Phys. Chem. A* **105**, 7371 (2001), <https://doi.org/10.1021/jp004317x>, URL <https://doi.org/10.1021/jp004317x>.
- [14] T. Yamada, T. Horita, K. Ouchi, and H. Fujisaka, *Prog. Theor. Phys.* **116**, 819 (2006), URL <http://dx.doi.org/10.1143/PTP.116.819>.
- [15] J. Buceta and K. Lindenberg, *Phys. Rev. E* **68**, 011103 (2003), URL <https://link.aps.org/doi/10.1103/PhysRevE.68.011103>.
- [16] D. Das and D. S. Ray, *Phys. Rev. E* **87**, 062924 (2013), URL <https://link.aps.org/doi/10.1103/PhysRevE.87.062924>.
- [17] F. Moss and P. McClintock, Noise in Nonlinear Dynamical Systems: Theory of noise induced processes in special applications, Cambridge books online (Cambridge University Press, 1989), ISBN 9780521352291, URL https://books.google.co.in/books?id=1SfYr-yk_6oC.
- [18] X. Zheng, B. ten Hagen, A. Kaiser, M. Wu, H. Cui, Z. Silber-Li, and H. Löwen, *Phys. Rev. E* **88**, 032304 (2013), URL <https://link.aps.org/doi/10.1103/PhysRevE.88.032304>.

- [19] K. Malakar, V. Jemseena, A. Kundu, K. V. Kumar, S. Sabhapandit, S. N. Majumdar, S. Redner, and A. Dhar, *J. Stat. Mech. Theory Exp.* **2018**, 043215 (2018), URL <http://stacks.iop.org/1742-5468/2018/i=4/a=043215>.
- [20] T. B. Kepler and T. C. Elston, *Biophys. J* **81**, 3116 (2001), ISSN 0006-3495, URL <http://www.sciencedirect.com/science/article/pii/S0006349501759498>.
- [21] J. E. M. Hornos, D. Schultz, G. C. P. Innocentini, J. Wang, A. M. Walczak, J. N. Onuchic, and P. G. Wolynes, *Phys. Rev. E* **72**, 051907 (2005), URL <https://link.aps.org/doi/10.1103/PhysRevE.72.051907>.
- [22] V. Shahrezaei and P. S. Swain, *Proc. Natl. Acad. Sci. U.S.A* (2008), ISSN 0027-8424, <http://www.pnas.org/content/early/2008/11/05/0803850105.full.pdf>, URL <http://www.pnas.org/content/early/2008/11/05/0803850105>.
- [23] S. Zeiser, U. Franz, and V. Liebscher, *J. Math. Biol.* **60**, 207 (2009), URL <https://doi.org/10.1007/s00285-009-0264-9>.
- [24] N. Kumar, T. Platini, and R. V. Kulkarni, *Phys. Rev. Lett.* **113**, 268105 (2014), URL <https://link.aps.org/doi/10.1103/PhysRevLett.113.268105>.
- [25] P. Thomas, N. Popović, and R. Grima, *Proc. Natl. Acad. Sci. U.S.A* **111**, 6994 (2014), ISSN 0027-8424, <http://www.pnas.org/content/111/19/6994.full.pdf>, URL <http://www.pnas.org/content/111/19/6994>.
- [26] A. Duncan, S. Liao, T. c. v. Vejchodský, R. Erban, and R. Grima, *Phys. Rev. E* **91**, 042111 (2015), URL <https://link.aps.org/doi/10.1103/PhysRevE.91.042111>.
- [27] D. A. Potoyan and P. G. Wolynes, *J. Chem. Phys* **143**, 11B612_1 (2015).
- [28] Q. Luo and X. Mao, *J. Math. Anal. Appl.* **334**, 69 (2007), ISSN 0022-247X, URL <http://www.sciencedirect.com/science/article/pii/S0022247X06013977>.
- [29] Q. Luo and X. Mao, *J. Math. Anal. Appl.* **355**, 577 (2009).
- [30] C. Zhu and G. Yin, *J. Math. Anal. Appl.* **357**, 154 (2009), ISSN 0022-247X, URL <http://www.sciencedirect.com/science/article/pii/S0022247X09002777>.
- [31] P. Ashcroft, P. M. Altrock, and T. Galla, *J. R. Soc. Interface* **11** (2014), ISSN 1742-5689, <http://rsif.royalsocietypublishing.org/content/11/100/20140663.full.pdf>, URL <http://rsif.royalsocietypublishing.org/content/11/100/20140663>.
- [32] K. Wienand, E. Frey, and M. Mobilia, *Phys. Rev. Lett.* **119**, 158301 (2017), URL <https://link.aps.org/doi/10.1103/PhysRevLett.119.158301>.

- [33] E. Kussell and S. Leibler, *Science* **309**, 2075 (2005).
- [34] E. L. Kussell, R. Kishony, N. Q. Balaban, and S. Leibler, *Genetics* (2005).
- [35] A. Argun, A.-R. Moradi, E. Pınçe, G. B. Bağcı, A. Imparato, and G. Volpe, *Phys. Rev. E* **94**, 062150 (2016), URL <https://link.aps.org/doi/10.1103/PhysRevE.94.062150>.
- [36] C. Maggi, M. Paoluzzi, N. Pellicciotta, A. Lepore, L. Angelani, and R. Di Leonardo, *Phys. Rev. Lett.* **113**, 238303 (2014), URL <https://link.aps.org/doi/10.1103/PhysRevLett.113.238303>.
- [37] M. Sandoval and L. Dagdug, *Phys. Rev. E* **90**, 062711 (2014), URL <https://link.aps.org/doi/10.1103/PhysRevE.90.062711>.
- [38] J. Tailleur and M. E. Cates, *EPL* **86**, 60002 (2009), URL <http://stacks.iop.org/0295-5075/86/i=6/a=60002>.
- [39] Y. Fily, A. Baskaran, and M. F. Hagan, *Phys. Rev. E* **91**, 012125 (2015), URL <https://link.aps.org/doi/10.1103/PhysRevE.91.012125>.
- [40] I. Rodriguez-Iturbe, A. Porporato, L. Ridolfi, V. Isham, and D. Coxi, in *Proc. R. Soc. London, Ser. A* (The Royal Society, 1999), vol. 455, pp. 3789–3805.
- [41] P. D’Odorico, F. Laio, and L. Ridolfi, *Am. Nat.* **167**, E79 (2006).
- [42] S. I. Denisov, W. Horsthemke, and P. Hänggi, *Eur. Phys. J. B* **68**, 567 (2009).
- [43] P. Hänggi and P. Jung, *Adv. Chem. Phys.* **89**, 239 (1994).
- [44] A. Kamenev, *Field theory of non-equilibrium systems* (Cambridge University Press, 2011).
- [45] D. Janakiraman and K. L. Sebastian, *Phys. Rev. E* **86**, 061105 (2012).
- [46] A. Morita, *Phys. Rev. A* **41**, 754 (1990), URL <https://link.aps.org/doi/10.1103/PhysRevA.41.754>.
- [47] V. I. Klyatskin, *Radiophys. Quantum Electron.* **20**, 382 (1977), ISSN 1573-9120, URL <https://doi.org/10.1007/BF01033925>.
- [48] I. BENA, *Int. J. Mod. Phys. A* **20**, 2825 (2006), URL <https://www.worldscientific.com/doi/abs/10.1142/S0217979206034881>.
- [49] K. Goswami, *Phys.Rev.E* **99**, 012112 (2019).
- [50] H. Bateman, A. Erdélyi, et al., *Higher transcendental functions*, vol. 2 (McGraw-Hill New York, 1953).
- [51] F. W. Olver, D. W. Lozier, R. F. Boisvert, and C. W. Clark, *NIST handbook of mathematical functions hardback and CD-ROM* (Cambridge university press, 2010).

- [52] C. Bechinger, R. Di Leonardo, H. Löwen, C. Reichhardt, G. Volpe, and G. Volpe, *Rev. Mod. Phys.* **88**, 045006 (2016), URL <https://link.aps.org/doi/10.1103/RevModPhys.88.045006>.
- [53] P. G. Hufton, Y. T. Lin, T. Galla, and A. J. McKane, *Phys. Rev. E* **93**, 052119 (2016).
- [54] D. Loi, S. Mossa, and L. F. Cugliandolo, *Phys. Rev. E* **77**, 051111 (2008), URL <https://link.aps.org/doi/10.1103/PhysRevE.77.051111>.
- [55] K. Goswami, *Physica A* **525**, 223 (2019), ISSN 0378-4371, URL <http://www.sciencedirect.com/science/article/pii/S0378437119302857>.
- [56] C. M. Bender and S. A. Orszag, Advanced mathematical methods for scientists and engineers I: Asymptotic methods and perturbation theory (Springer Science & Business Media, 2013).